Electronic Supplementary Material (ESI) for Chemical Science.
This journal is © The Royal Society of Chemistry 2022

Acene Enlargement for Absorption Red-Shifting and Photosensitization Enhancement of Photosensitizers with Aggregation-Induced Emission

Qiang Wang[a], Chunbin Li[b], Yuchen Song[a], Qiankun Shi[a], Heng Li[c], Hua Zhong[c,*], Jianguo Wang[b,*], and Fang Hu[a,*]

[a] Guangdong Provincial Key Laboratory of Construction and Detection in Tissue Engineering, Biomaterials Research Center, School of Biomedical Engineering, Southern Medical University, Guangzhou 510515, China.

[b] College of Chemistry and Chemical Engineering, Inner Mongolia Key Laboratory of Fine Organic Synthesis, Inner Mongolia University, Hohhot 010021, China.

[c] Department of Orthopaedics, The Fifth Affiliated Hospital, Southerm Medical University, Guangzhou 510900, China.

Experimental Procedures

Materials and instrumentation

Bis(4-bromophenyl)fumaronitrile, *N*-phenylnaphthalen-2-amine, $Pd(OAc)_2$, $(t\text{-}Bu)_3P$, and aniline were purchased from Macklin; 4,4'-dimethoxydiphenylamine, diphenylamine, 2-bromoanthracene, and Cs_2CO_3 were purchased from Bidepharm; $Pd(dba)_3$ was purchased from Adamas; DSPE-PEG_{2000}, Chlorin E6 (Ce6) and 2',7'-dichlorodihydrofluorescein (DCFH) was purchased from Yuanye biotechnology; 9,10-anthracenediyl-bis(methylene)dimalonic acid (ABDA) were purchased from Sigma; 2',7'-dichlorofluorescein diacetate (DCFH-DA), 3-(4,5-dimethylthiazol-2-yl)-2,5-diphenyltetrazolium bromide (MTT), and Calcein-AM (CAM)/PI Double Stain Kit were provided by Solarbio. Compounds TFN, MeO-TFN [1], Nap-TFN [2], were synthesized according to reported literature. All other chemicals were obtained from commercial sources and used as received without further purification.

^1H NMR spectra and ^{13}C NMR spectra were recorded on a 400 MHz Bruker AVANCE III spectrometer. Electrospray ionization mass spectrometry (ESI-MS) was carried out on an LC-MS (Thermo Scientific, USA) system. Hydrodynamic diameter and size distribution were measured on a Malvern Nano ZS dynamic light scattering (DLS) and transmission electron microscopy (TEM) with JEOL-1400 PLUS. Cytotoxicity tests were carried out on a microplate reader (Biotek Synergy HT) by using MTT assays. The LWGL530-2W and optical power meter are suplied by Beijing Laserwave OpoElectronics Technology Co., Ltd. Confocal Laser Scanning Microscopy (CLSM) images were recorded by NIS-Elements 5.3 (Nikon). The PDT experiments were carried out by a GR-60WL cold white light source.

Synthetic procedure

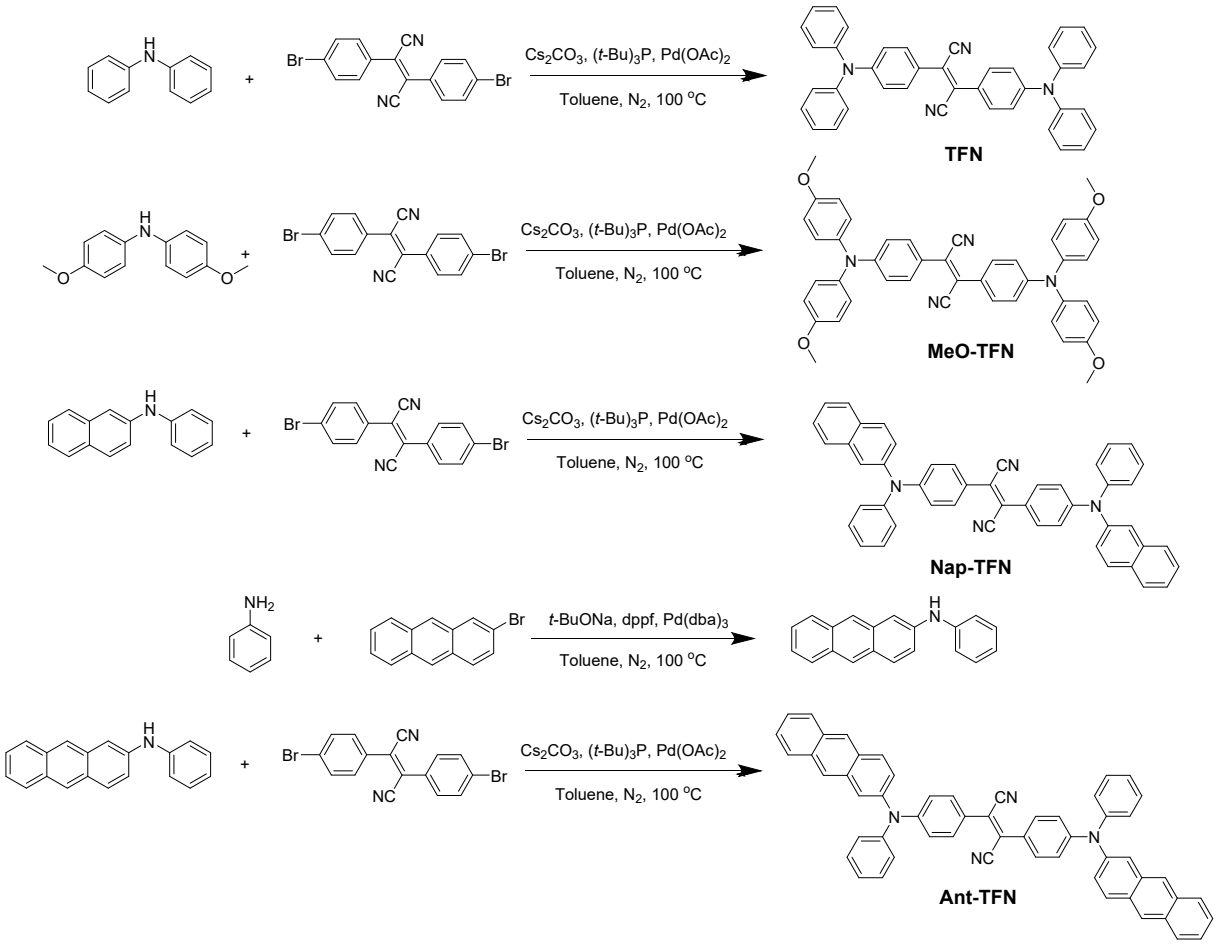

Scheme S1. The synthetic routes to TFN, MeO-TFN, Nap-TFN, and Ant-TFN.

Synthesis of compound TFN: Under N_2 atmosphere, a solution of bis(4-bromophenyl)fumaronitrile (154.4 mg, 0.4 mmol) in toluene (15 mL) was injected in diphenylamine (169.2 mg, 1 mmol), Cs_2CO_3 (909.9 mg, 2.79 mmol), (t-Bu)$_3$P (24.3 mg, 0.12 mmol), $Pd(OAc)_2$ (8.9 mg, 0.04 mmol) and then the mixture was heated to 100 °C for 16 hours. The mixed solution was extracted with CH_2Cl_2 and H_2O. The combined organic layer was dried over anhydrous Na_2SO_4 and evaporated under reduced pressure. The residue was purified on silica gel with petroleum ether/CH_2Cl_2 (1:1, *v*/*v*) to afford compound **TFN** as a red solid. Yield: 80%. ^{1}H NMR (400 MHz, $CDCl_3$) δ 7.69 (dd, J = 15.7, 6.9 Hz, 4H), 7.34 (dd, J = 16.2, 8.6 Hz, 8H), 7.28 – 7.12 (m, 14H), 7.07 (d, J = 8.8 Hz, 4H).

Synthesis of compound MeO-TFN: Under N_2 atmosphere, a solution of bis(4-bromophenyl)fumaronitrile (154.4 mg, 0.4 mmol) in toluene (15 mL) was injected in 4,4'-Dimethoxydiphenylamine (229.2 mg, 1 mmol), Cs_2CO_3 (909.9 mg, 2.79 mmol), (t-Bu)$_3$P (24.3 mg, 0.12

mmol), $Pd(OAc)_2$ (8.9 mg, 0.04 mmol) and then the mixture was heated to 100 °C for 16 hours. The mixed solution was extracted with CH_2Cl_2 and H_2O. The combined organic layer was dried over anhydrous Na_2SO_4 and evaporated under reduced pressure. The residue was purified on silica gel with petroleum ether/CH_2Cl_2 (1:1, *v*/*v*) to afford compound **MeO-TFN** as a dark red solid. Yield: 85%. ^{1}H NMR (400 MHz, $CDCl_3$) δ 7.61 (d, J = 8.4 Hz, 4H), 7.12 (d, J = 8.0 Hz, 8H), 6.88 (d, J = 8.2 Hz, 12H), 3.81 (s, 12H).

Synthesis of compound Nap-TFN: Under N_2 atmosphere, a solution of bis(4-bromophenyl)fumaronitrile (154.4 mg, 0.4 mmol) in toluene (15 mL) was injected in *N*-phenylnaphthalen-2-amine (219.1 mg, 1 mmol), Cs_2CO_3 (909.9 mg, 2.79 mmol), (t-Bu)$_3$P (24.3 mg, 0.12 mmol), $Pd(OAc)_2$ (8.9 mg, 0.04 mmol) and then the mixture was heated to 100 °C for 16 hours. The mixed solution was extracted with CH_2Cl_2 and H_2O. The combined organic layer was dried over anhydrous Na_2SO_4 and evaporated under reduced pressure. The residue was purified on silica gel with petroleum ether/CH_2Cl_2 (1:1, *v*/*v*) to afford compound **Nap-TFN** as a red solid. Yield: 83%. ^{1}H NMR (400 MHz, $CDCl_3$) δ 7.80 (dd, J = 15.3, 7.1 Hz, 4H), 7.73 – 7.66 (m, 8H), 7.65 (d, J = 3.8 Hz, 2H), 7.57 (d, J = 9.2 Hz, 2H), 7.48 – 7.40 (m, 3H), 7.33 (dd, J = 15.3, 7.9 Hz, 5H), 7.19 (dt, J = 14.6, 6.4 Hz, 5H), 7.11 (d, J = 7.7 Hz, 3H).

Synthesis of compound N-phenylanthracen-2-amine: Under N_2 atmosphere, a solution of 2-bromoanthracene (1028.5 mg, 4 mmol) in toluene (30 mL) was injected in aniline (558.7 mg, 6 mmol), *t*-BuONa (576.6 mg, 6 mmol), $Pd(dba)_3$ (39.0 mg, 0.04 mmol), dppf (44.4 mg, 0.08 mmol) and then the mixture was heated to 100 °C for 12 hours. The mixed solution was extracted with CH_2Cl_2 and H_2O. The combined organic layer was dried over anhydrous Na_2SO_4 and evaporated under reduced pressure. The residue was purified on silica gel with petroleum ether/CH_2Cl_2 (2:1, *v*/*v*) to afford *N*-phenylanthracen-2-amine as a yellow solid. Yield: 80%. ^{1}H NMR (400 MHz, $CDCl_3$) δ 8.30 (s, 1H), 8.16 (s, 1H), 7.91 (dd, J = 16.5, 7.5 Hz, 3H), 7.53 (s, 1H), 7.45 – 7.30 (m, 4H), 7.22 (d, J = 8.4 Hz, 3H), 7.02 (t, J = 7.3 Hz, 1H).

Synthesis of compound Ant-TFN: *N*-Phenylanthracen-2-amine (269.3 mg, 1 mmol), Cs_2CO_3 (909.9 mg, 2.79 mmol), (t-Bu)$_3$P (24.3 mg, 0.12 mmol) and $Pd(OAc)_2$ (8.9 mg, 0.04 mmol) were added into the solution of bis(4-bromophenyl)fumaronitrile (154.4 mg, 0.4 mmol) in toluene (15 mL). The mixture was heated to 100 °C for 16 hours under a nitrogen atmosphere. After cooling to 25 °C, the mixed solution was poured into water (150 mL) and extracted with CH_2Cl_2 (100 mL × 3). The combined organic layer was dried over anhydrous Na_2SO_4 and evaporated under reduced pressure. The residue was purified on silica gel with petroleum ether/CH_2Cl_2 (1:1, *v*/*v*) to afford **Ant-TFN** as a red solid. Yield: 50%. ^{1}H NMR (400 MHz, $CDCl_3$) δ 8.37 (s, 2H), 8.21 (s, 2H), 7.9 (dt, J = 9.2, 6.0 Hz, 6H), 7.73 (d, J = 8.8 Hz, 4H),

7.66 (s, 2H), 7.48-7.41 (m, 4H), 7.37 (t, J = 7.8 Hz, 4H), 7.30 (dd, J = 9.1, 1.9 Hz, 3H), 7.25 (d, J = 2.9 Hz, 3H), 7.19 (dd, J = 12.7, 8.1 Hz, 6H). ^{13}C NMR (101 MHz, $CDCl_3$) δ 150.2, 146.2, 143.3, 132.2, 131.4, 129.9, 129.8, 129.4, 128.2, 127.9, 126.1, 125.7, 125.2, 125.1, 125.0, 121.6, 121.2, 117.7. ESI-MS, m/z: [M] calcd 764.3, found 764.1.

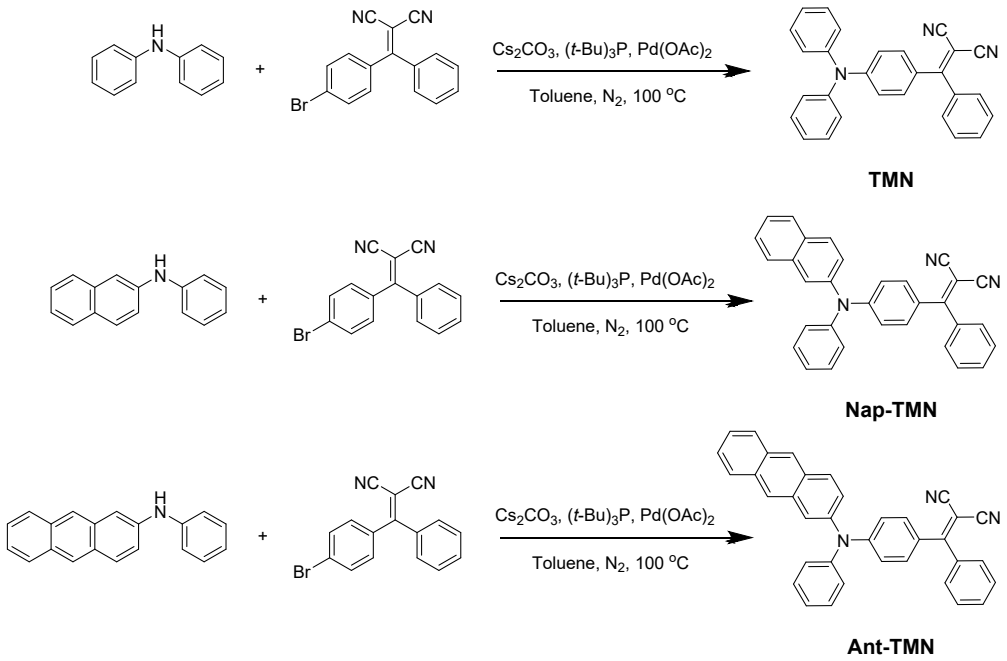

Scheme S2. The synthetic routes to TMN, Nap-TMN, and Ant-TMN.

Synthesis of compound TMN: Under N_2 atmosphere, a solution of 2-((4-bromophenyl)(phenyl)methylene)malononitrile (123.6 mg, 0.4 mmol) in toluene (15 mL) was injected in diphenylamine (67.6 mg, 0.4 mmol), Cs_2CO_3 (909.9 mg, 2.79 mmol), (t-Bu)$_3$P (24.3 mg, 0.12 mmol), $Pd(OAc)_2$ (8.9 mg, 0.04 mmol) and then the mixture was heated to 100 °C for 16 hours. The mixed solution was extracted with CH_2Cl_2 and H_2O. The combined organic layer was dried over anhydrous Na_2SO_4 and evaporated under reduced pressure. The residue was purified on silica gel with petroleum ether/CH_2Cl_2 (1:1, v/v) to afford compound **TMN** as a red solid. Yield: 70%. ^{1}H NMR (400 MHz, $CDCl_3$) δ 7.91 – 7.76 (m, 1H), 7.58 – 7.52 (m, 1H), 7.45 (dt, J = 8.6, 4.7 Hz, 4H), 7.34 (dd, J = 16.8, 8.6 Hz, 6H), 7.23 – 7.13 (m, 5H), 6.92 (d, J = 9.0 Hz, 2H). ^{13}C NMR (101 MHz, $CDCl_3$) δ 173.5, 152.3, 145.6, 136.6, 132.6, 132.1, 131.9, 130.4, 130.2, 130.0, 129.8, 128.6, 126.6, 126.5, 125.5, 118.3, 115.2, 114.9, 77.2.

Synthesis of compound Nap-TMN: Under N_2 atmosphere, a solution of 2-((4-bromophenyl)(phenyl)methylene)malononitrile (123.6 mg, 0.4 mmol) in toluene (15 mL) was injected in *N*-phenylnaphthalen-2-amine (87.6 mg, 0.4 mmol), Cs_2CO_3 (909.9 mg, 2.79 mmol), (*t*-Bu)$_3$P (24.3 mg, 0.12 mmol), $Pd(OAc)_2$ (8.9 mg, 0.04 mmol) and then the mixture was heated to 100 °C for 16 hours. The mixed solution was extracted with CH_2Cl_2 and H_2O. The combined organic layer was dried over anhydrous Na_2SO_4 and evaporated under reduced pressure. The residue was purified on silica gel with petroleum ether/CH_2Cl_2 (1:1, *v*/*v*) to afford compound **Nap-TMN** as a red solid. Yield: 83%. ^{1}H NMR (400 MHz, $CDCl_3$) δ 7.90 – 7.76 (m, 2H), 7.71 – 7.66 (m, 1H), 7.60 (d, J = 1.6 Hz, 1H), 7.58 – 7.51 (m, 1H), 7.46 (dt, J = 10.0, 7.3 Hz, 6H), 7.40 – 7.29 (m, 5H), 7.21 (dd, J = 16.0, 7.7 Hz, 3H), 6.99 (d, J = 8.9 Hz, 2H). ^{13}C NMR (101 MHz, $CDCl_3$) δ 173.5, 152.2, 145.7, 143.1, 136.6, 134.1, 132.6, 132.0, 131.2, 130.4, 129.8, 129.7, 128.7, 127.7, 127.3, 127.0, 126.6, 126.5, 125.8, 125.6, 125.2, 123.8, 118.7, 115.1, 114.8, 77.2.

Synthesis of compound Ant-TMN: Under N_2 atmosphere, a solution of 2-((4-bromophenyl)(phenyl)methylene)malononitrile (123.6 mg, 0.4 mmol) in toluene (15 mL) was injected in *N*-Phenylanthracen-2-amine (107.72 mg, 0.4 mmol), Cs_2CO_3 (909.9 mg, 2.79 mmol), (*t*-Bu)$_3$P (24.3 mg, 0.12 mmol), $Pd(OAc)_2$ (8.9 mg, 0.04 mmol) and then the mixture was heated to 100 °C for 16 hours. The mixed solution was extracted with CH_2Cl_2 and H_2O. The combined organic layer was dried over anhydrous Na_2SO_4 and evaporated under reduced pressure. The residue was purified on silica gel with petroleum ether/CH_2Cl_2 (1:1, *v*/*v*) to afford compound **Ant-TMN** as a red solid. Yield: 85%. ^{1}H NMR (400 MHz, $CDCl_3$) δ 8.38 (s, 1H), 8.23 (s, 1H), 8.04 – 7.88 (m, 3H), 7.71 (s, 1H), 7.61 – 7.42 (m, 7H), 7.38 (dd, J = 14.4, 8.4 Hz, 4H), 7.33 – 7.27 (m, 3H), 7.23 (s, 1H), 7.05 (d, J = 8.9 Hz, 2H). ^{13}C NMR (101 MHz, $CDCl_3$) δ 173.5, 152.0, 145.6, 142.5, 136.7, 132.6, 132.1, 132.0, 132.0, 131.6, 130.4, 130.0, 129.9, 129.5, 128.7, 128.2, 127.9, 127.2, 126.6, 126.2, 125.9, 125.7, 125.4, 125.4, 125.0, 122.8, 119.1, 115.1, 114.8, 77.2.

Preparation of nanoparticles: The mixed THF solution (1 mL) containing TFN, MeO-TFN, Nap-TFN or Ant-TFN (1 mg) and DSPE-PEG_{2000} (3 mg) was rapidly injected into water (10 mL) under sonication. After continuous sonication for 5 minutes, THF was evaporated by stirring at room temperature overnight. The obtained NPs were filtered through a 0.22 μm syringe filter and stored in the dark at 4 °C.

Singlet oxygen production evaluation: To evaluate the singlet oxygen generation ability of photosensitizers (PSs), a chemical method using 9,10-anthracenediyl-bis(methylene)dimalonic acid (ABDA) was employed with UV-*vis* spectroscopy. PSs dissolved in water (10 μM, 1 mL) were blended

with an ABDA solution (100 μM) and then irradiated with 60 mW cm^{-2} of white light. The absorption intensity of the ABDA at the maximum wavelength of 378 nm was detected every 1 min. To compare the reactive oxygen species (ROS) generation ability of photosensitizers (PSs) with Ce6, ROS fluorescence probe 2',7'-dichlorodihydrofluorescein (DCFH) was employed with fluorescent spectrometry. PSs (10 μM) or Ce6 (10 μM) dissolved in water were blended with DCFH solution (5 μM) and then irradiated with 60 mW cm^{-2} of white light. The fluorescence intensity of the DCFH at the maximum emission wavelength of 523 nm was detected every 10 s.

Measurement of fluorescence quantum yield: The fluorescence quantum yield (Φ) of the TFN, MeO-TFN, Nap-TFN, and Ant-TFN in aqueous media were measured using a standard fluorescence comparison method. Freshly prepared 4-(dicyanomethylene)-2-methyl-6-(4-dimethylaminostyryl)-4*H*-pyran (DCM) in methanol was used as reference (Φ=43.3%). The UV-*vis* absorption spectra of compounds in aqueous media and DCM in methanol were measured and the maximum absorption was limited to less than 0.1 to minimize the self-absorption effect. The fluorescence spectra then were recorded under maximum excitation. The fluorescence intensities were obtained through wavelength integration. The fluorescence quantum yield (Φ) of AIE PSs was calculated by the following equation:

$$\Phi_x = \Phi_{st}\left(\frac{k_x}{k_{st}}\right)\left(\frac{\eta_x^2}{\eta_{st}^2}\right)$$

where Φ_{st} is the standard fluorescence quantum yield (Φ_{DCM}=43.3%). k_x and k_{st} are is the slope after linear fitting of fluorescence intensity integral *vs.* the absorption of AIE PSs and DCM, respectively. η_x and η_{st} are the refractive indexes of the solvent. The subscripts x and st denote the sample and the reference (DCM in methanol).

Computational details: All molecules were fully optimized by the hybrid B3LYP, in combination with the 6-311G(d) basis set. The excited-state characteristics were calculated by time-dependent density functional theory (TD-DFT) using optimized ground state geometries. TD-DFT in combination with the B3LYP hybrid functional method and the 6-311G(d) basis set has been shown to provide accurate energies for the excited state of D-A molecular systems.

Cell cultures: The Murine breast cancer (4T1) cells were cultured in DMEM (containing 10% heat-inactivated fetal bovine serum and 1% Penicillin streptomycin) at 37 °C in a humidified incubator with 5% CO_2. Before the experiments, the cells were pre-cultured until confluence was reached.

Intracellular reactive oxygen species (ROS) detection: 4T1 cells were seeded and cultured for 24 h. The cells were treated with 20 μg/mL TFN NPs, MeO-TFN NPs, Nap-TFN NPs, or Ant-TFN NPs. After incubation for 8 h, all of the cells were washed with PBS and treated with 2,7-dichlorofluorescein diacetate (DCFH-DA) (5 μM) for 30 min. After that, the cells in light groups were irradiated with 60 mW cm^{-2} of white light for 12 min, while the other cells were incubated in the dark. The cellular fluorescence was observed by CLSM to evaluate the intracellular ROS production.

Live-dead cell staining: 4T1 cells were treated with 20 μg/mL TFN NPs, MeO-TFN NPs, Nap-TFN NPs, or Ant-TFN NPs for 8 h. Subsequently, the cells were irradiated with 60 mW cm^{-2} of white light for 12 min or incubated in the dark. After the treatment, the cells were further cultured for 4 h. Finally, the cells were washed by PBS and stained with Calcein-AM/PI for 30 min, and the residual dyes were washed out by PBS for three times. The green fluorescence of Calcein-AM and the red fluorescence of PI were observed by CLSM to evaluate the live and dead cells, respectively.

Cell viability: Cell viability was determined by using the MTT assay which is based on the reduction of 3-(4,5-dimethythiazol-2-yl)-2,5-diphenyl tetrazolium bromide (MTT) into formazan by mitochondrial succinate dehydrogenase. Dispense 100 μL of cell suspension (5000 cells/well) in a 96-well plate in DMEM (complemented with 1% penicillin/streptomycin and 10% FBS). Pre-incubate the plate for 24 h at 37 °C in a humidified incubator with 5% CO_2. Then 100 μL DMEM containing different concentrations of NPs (ranging from 0 to 40 μg/mL) was introduced to a 96-well plate. 8 hours later, the cells were treated with or without 60 mW cm^{-2} of white light for 12 min and then 4T1 cells were cultured for the next 24 hours. After that, 20 μL of freshly prepared MTT (5 mg/mL) solution was added to each well after the incubation period of 4 hours followed by the addition of 150 μL of DMSO to dissolve the formazan crystals. Absorbance was taken at 490 nm by a microplate reader.

Hemolysis assay: Fresh whole blood was collected from healthy female BALB/c mice in an anti-coagulation tube and was isolated by centrifuging at 4000 rpm for 10 min to obtain red blood cells (RBCs). RBCs were washed with PBS buffer until the supernatant was colorless. RBCs were then adjusted to a concentration of 4% RBCs solutions by PBS buffer. Next, 0.5 mL of the above RBCs were mixed with 0.5 mL of nanoparticles suspension to obtain different concentrations ranging from 0 to 100 μg/mL, respectively. All of the above samples were put into a constant temperature shaker at 37 ^{o}C for 3 h. After the supernatant of each sample was collected through centrifuging at 4000 rpm for 10 min, 100 μL of the above supernatant sample was added to a 96-well plate. The absorption of the supernatant sample was measured at 540 nm using a microplate reader. To avoid the absorption influence of nanoparticles themselves, the absorption of the same concentration of nanoparticles without RBCs was measured to act

as the negative control. A 0.5 ml 2% Triton X-100 PBS buffer (red blood cell lysis buffer) was mixed with 0.5 ml 4% RBCs to act as a positive control. The Hemolysis rate was calculated by the following equation:

$$\text{Hemolysis}(\%) = (A_{sam} - A_{neg}) / A_{pos} \times 100\%$$

A_{sam} is the absorption of sample (nanoparticles + RBCs); A_{neg} is the absorption of negative control (only nanoparticles); A_{pos} is positive control (nanoparticles + Triton X-100).

Antitumor study in *vivo*: All the animal experiments were approved by the laboratory animal research center of Southern Medical University (permit number: SYXK 2016-0041). The tumor model was established by subcutaneously injecting 4T1 cells onto the left hind leg of female BALB/c mice. Then the obtained 4T1 tumor-bearing mice were randomly divided into four groups and there were 5 mice in each group. When the tumors grew to about 80 mm^3, the mice were intravenously injected with PBS or Ant-TFN NPs (5 mg/kg) in different treatment groups. After 24 h, the mice in light groups were exposed to white light for 12 min at 300 mW cm^{-2}. The body weight and tumor volume were monitored every two days. After 14 days, the heart, liver, spleen, lung, kidney, and tumor tissues were harvested for H&E staining.

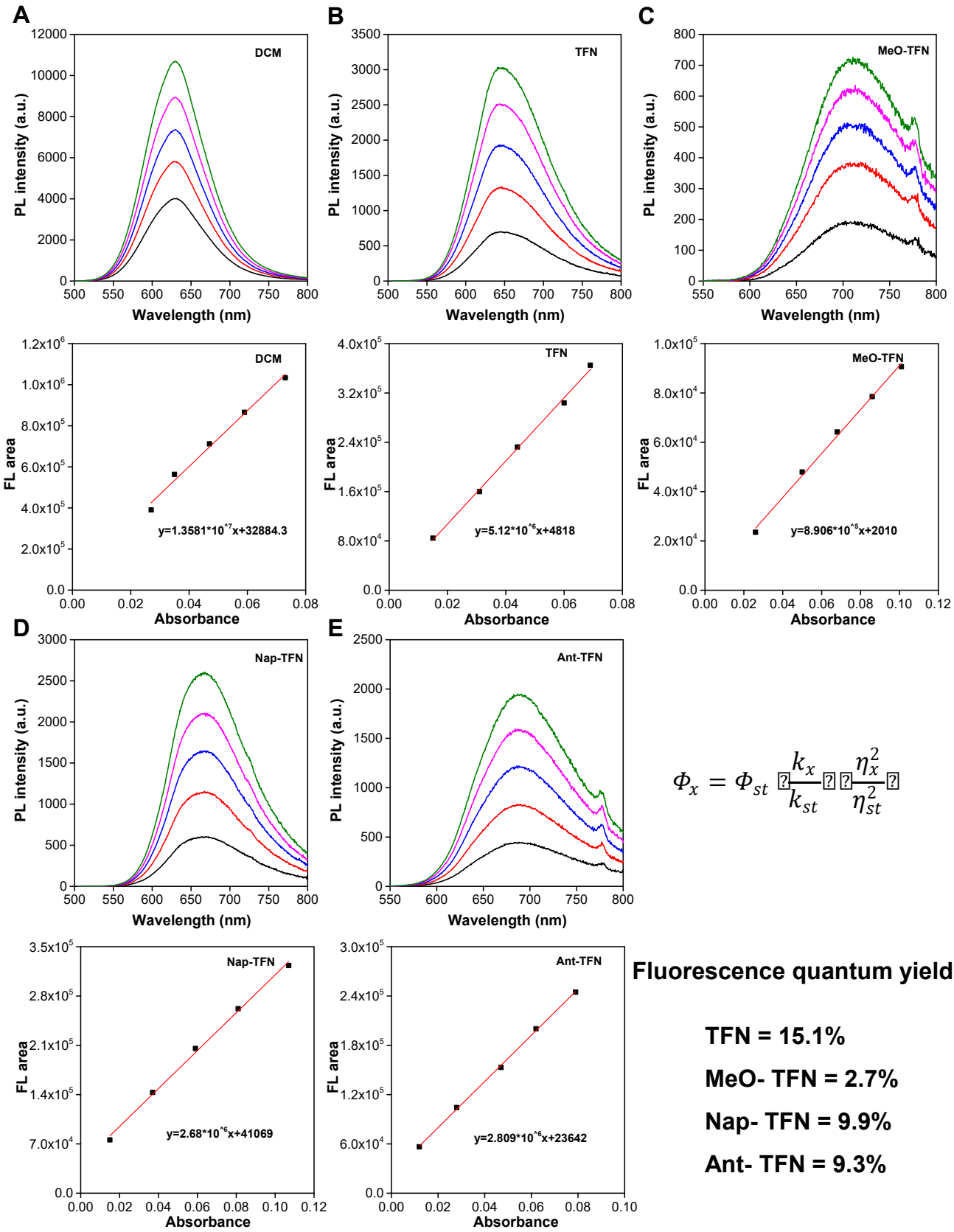

Figure S1. The fluorescence intensities of (A) DCM, (B) TFN, (C) MeO-TFN, (D) Nap-TFN, and (E) Ant-TFN with different absorption values, and the linear fitting of the fluorescence intensity integral *vs.* the relevant absorption values.

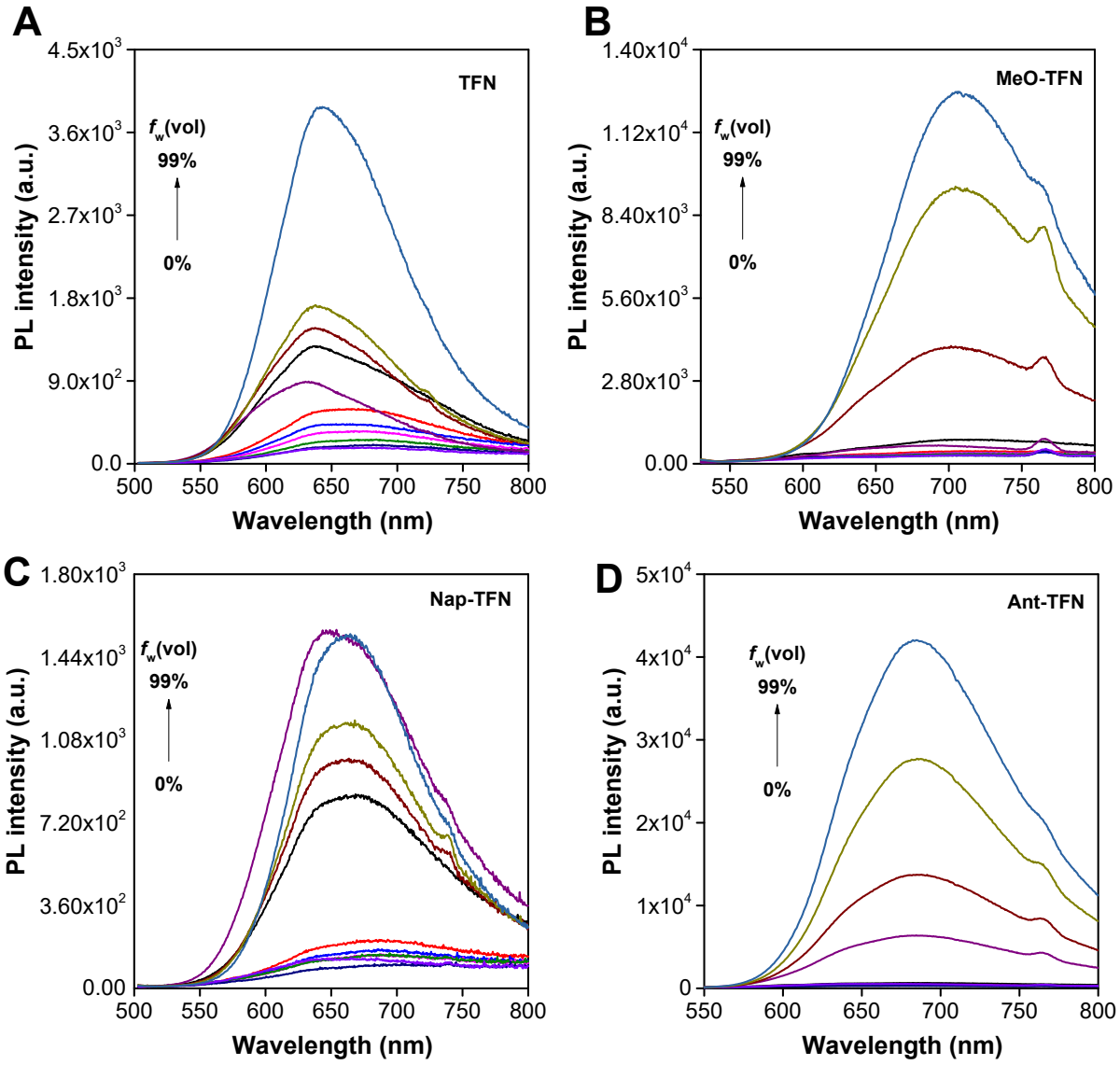

Figure S2. (A) Fluorescence spectra of TFN, (B) MeO-TFN, (C) Nap-TFN, and (D) Ant-TFN in water/THF mixtures with different water fractions (f_w). Excitation wavelength λ_{ex} = 482 nm for TFN, λ_{ex} = 514 nm for MeO-TFN, λ_{ex} = 497 nm for Nap-TFN, and λ_{ex} = 511 nm for Ant-TFN.

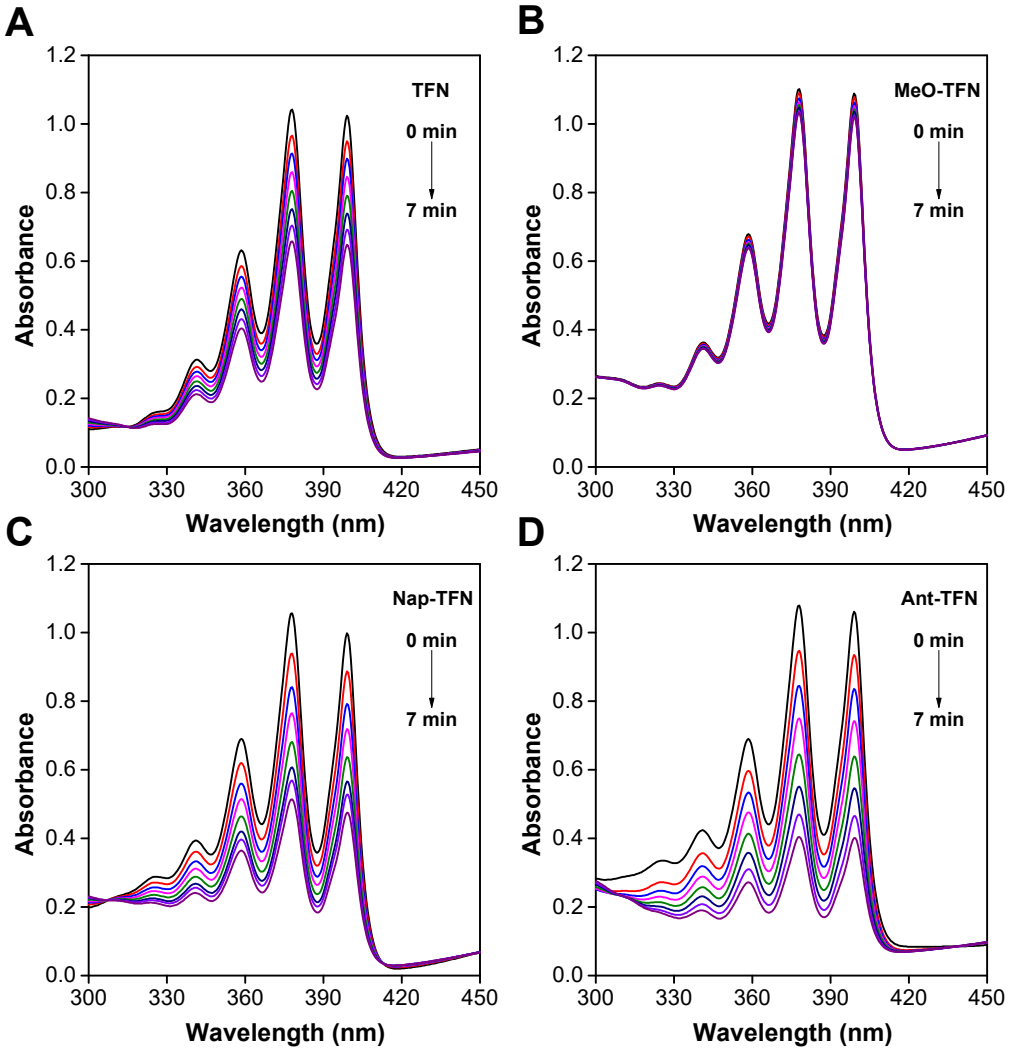

Figure S3. Absorption spectra of mixed solution of ABDA (100 μM) in DMSO:water = 1:99 with (A) TFN, (B) MeO-TFN, (C) Nap-TFN and (D) Ant-TFN (the concentration of all AIE PSs = 10 μM) under different time with 60 mW cm^{-2} white light irradiation.

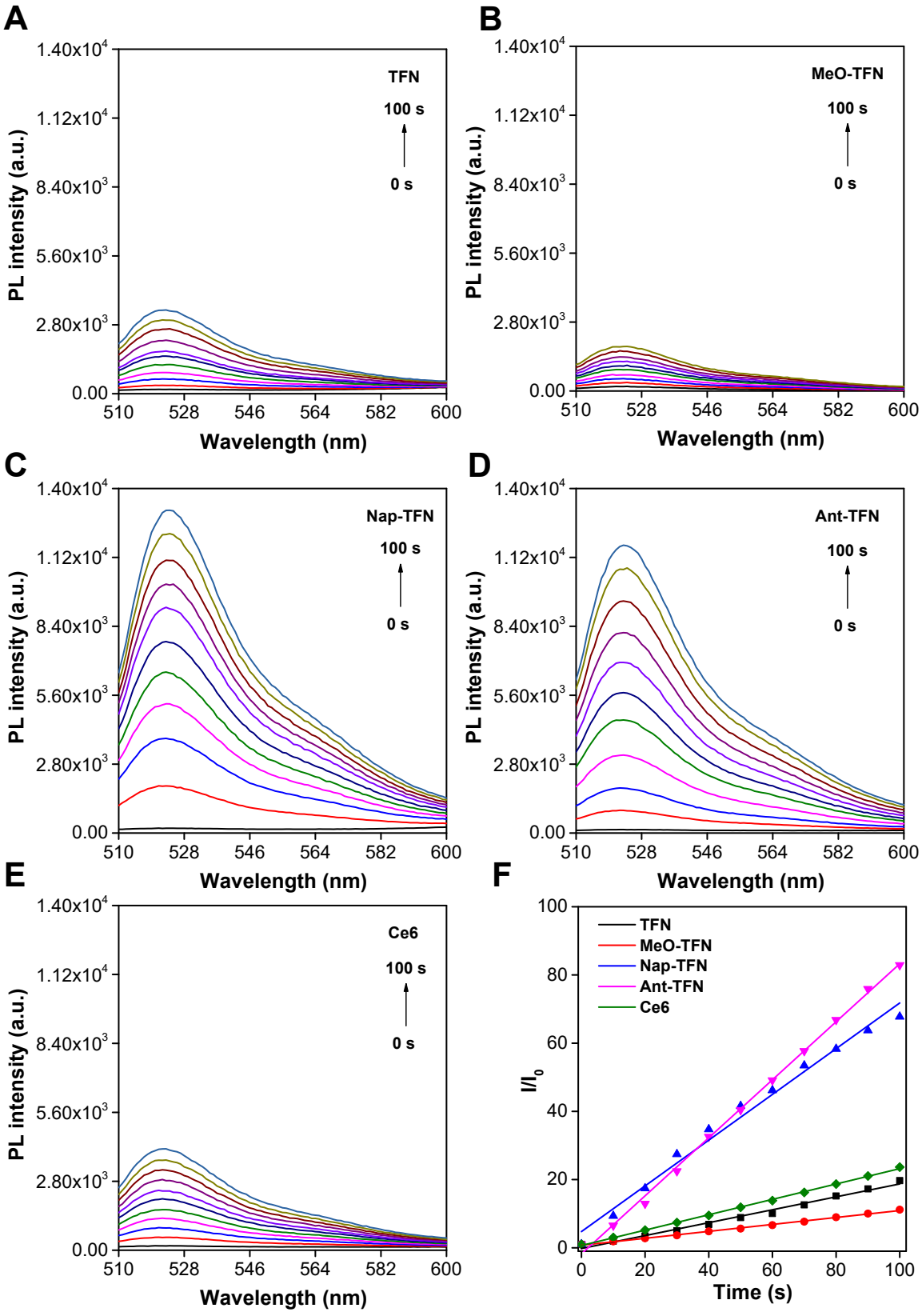

Figure S4. Fluorescence spectra of the mixed aqueous solution of DCFH (5 μM) with (A) TFN, (B) MeO-TFN, (C) Nap-TFN, (D) Ant-TFN, and (E) Ce6 under white light (60 mW cm^{-2}) irradiation. (Concentration of all photosensitizers = 10 μM). (F) Relative fluorescence intensities of TFN, MeO-TFN, Nap-TFN, Ant-TFN, and Ce6 at 523 nm with different irradiation times.

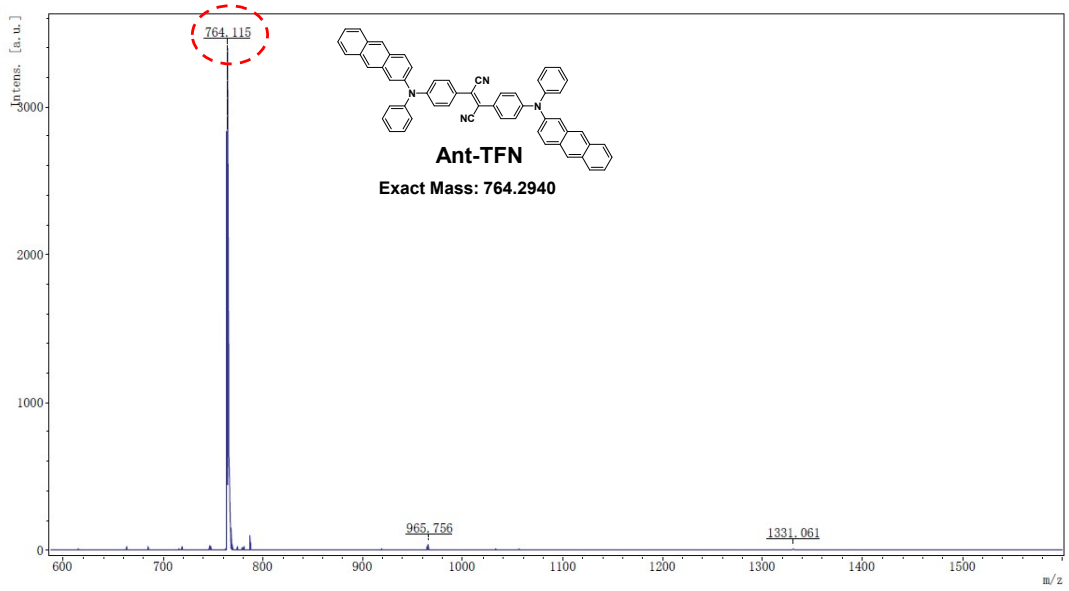

Figure S5. Mass spectrum of Ant-TFN.

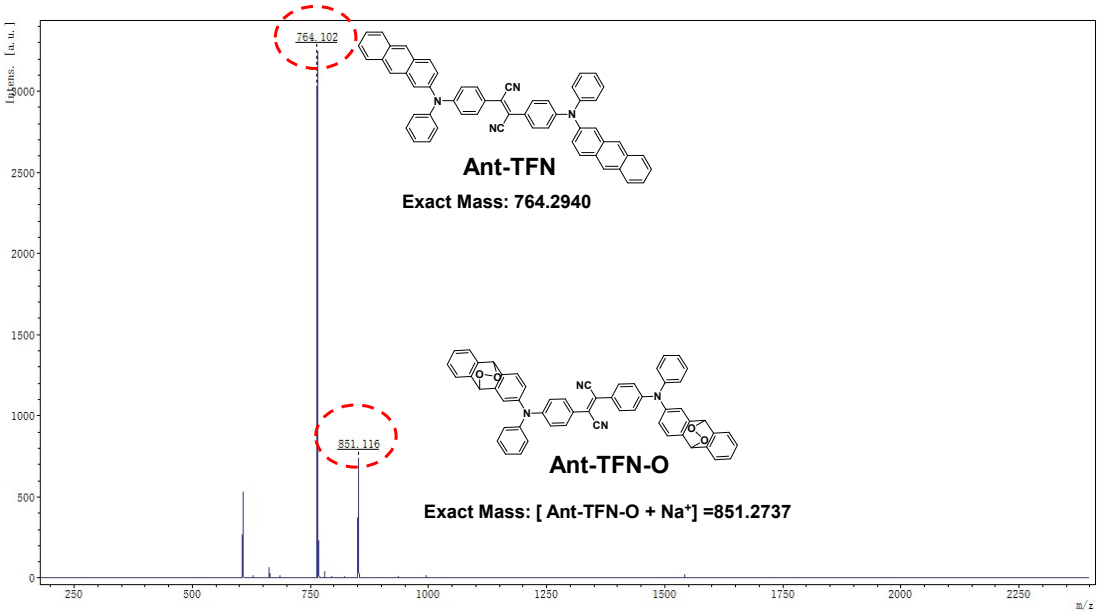

Figure S6. Mass spectrum of Ant-TFN after light irradiation for 12 min (350 mW cm^{-2}).

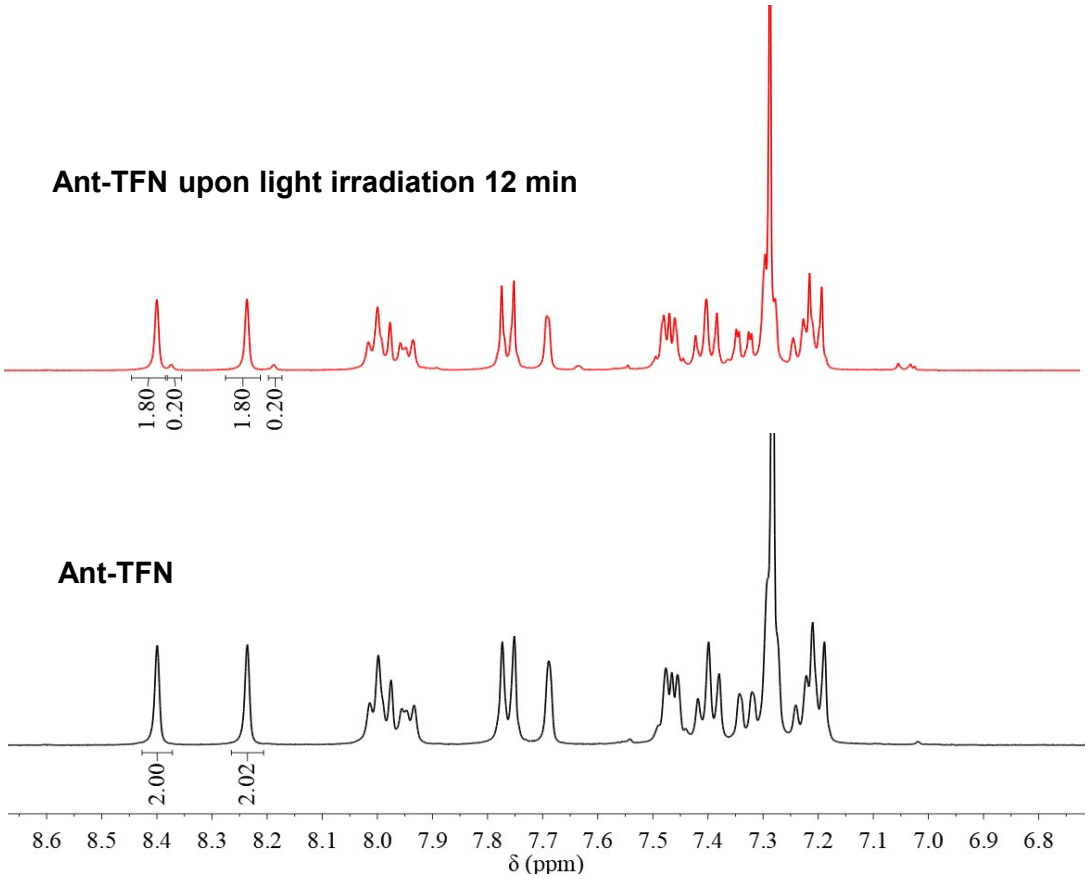

Figure S7. ^{1}H NMR spectral change (400 MHz) of Ant-TFN after light irradiation for 12 min (350 mW cm^{-2}).

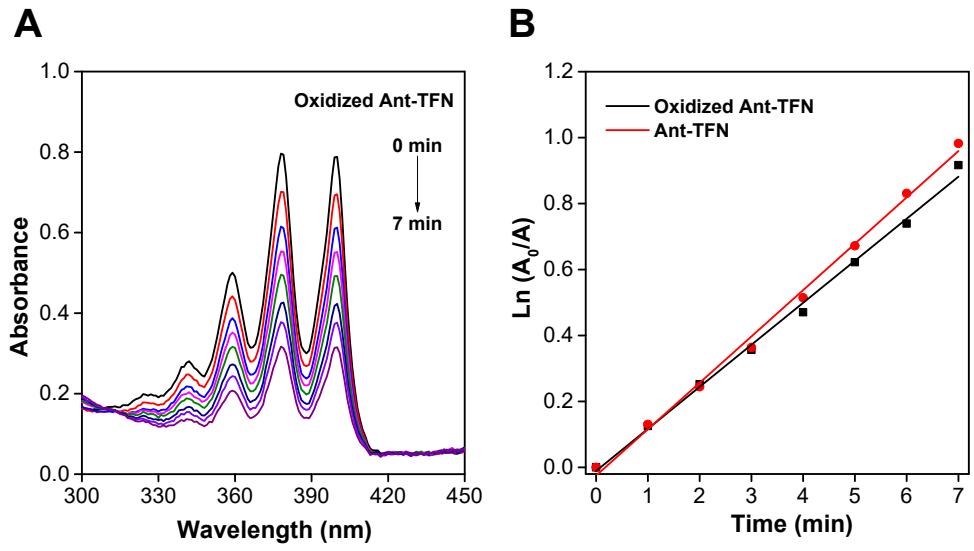

Figure S8. After light irradiation for 12 min (350 mW cm^{-2}), oxidized Ant-TFN decompose ABDA (100 μM) in DMSO: water = 1:99 under white light irradiation (60 mW cm^{-2}, 7 min). (B) Decomposition rates of ABDA of oxidized Ant-TFN and Ant-TFN.

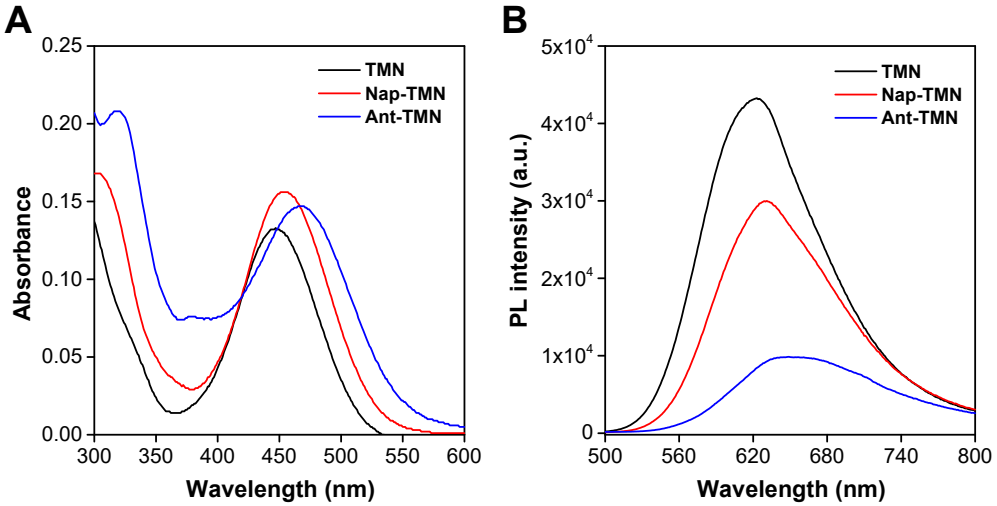

Figure S9. Optical properties. Absorption (A) and fluorescence (B) spectra of TMN, Nap-TMN, and Ant-TMN (10 μM) in DMSO/water (1/99, *v*/*v*). (λ_{ex} = 446 nm for TMN, λ_{ex} = 453 nm for Nap-TMN, λ_{ex} = 467 nm for Ant-TMN).

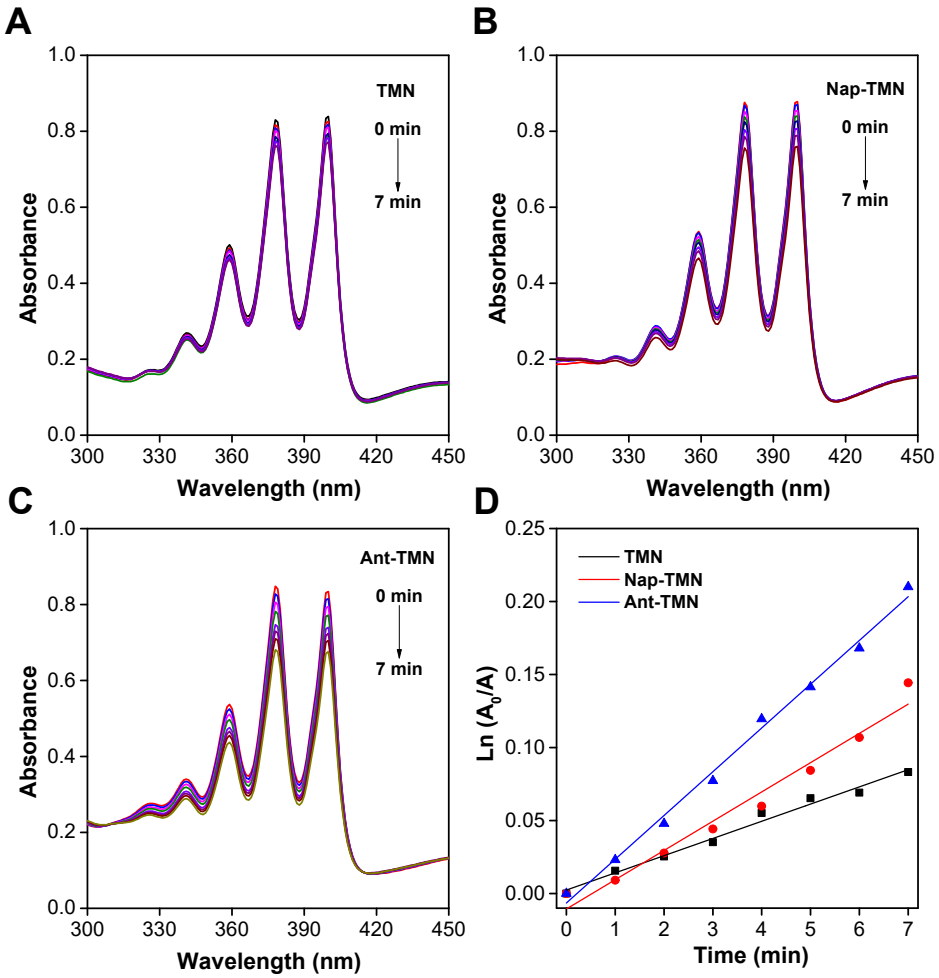

Figure S10. Absorption spectra of mixed solution of ABDA (100 μM) in DMSO: water = 1:99 with (A) TMN, (B) Nap-TMN, and (D) Ant-TMN (the concentration of all AIE PSs = 10 μM) under different time with 60 mW cm^{-2} white light irradiation.

Table S1. The summary of the optical properties of TMN, Nap-TMN, Ant-TMN.

PS	λ_{ex} (nm)	λ_{em} (nm)	$^1O_2$ production[a]
TMN	446	622	1
Nap-TMN	453	631	1.78
Ant-TMN	467	650	2.55

[a] Relative $^1O_2$ production capacities by referencing TMN aggregates.

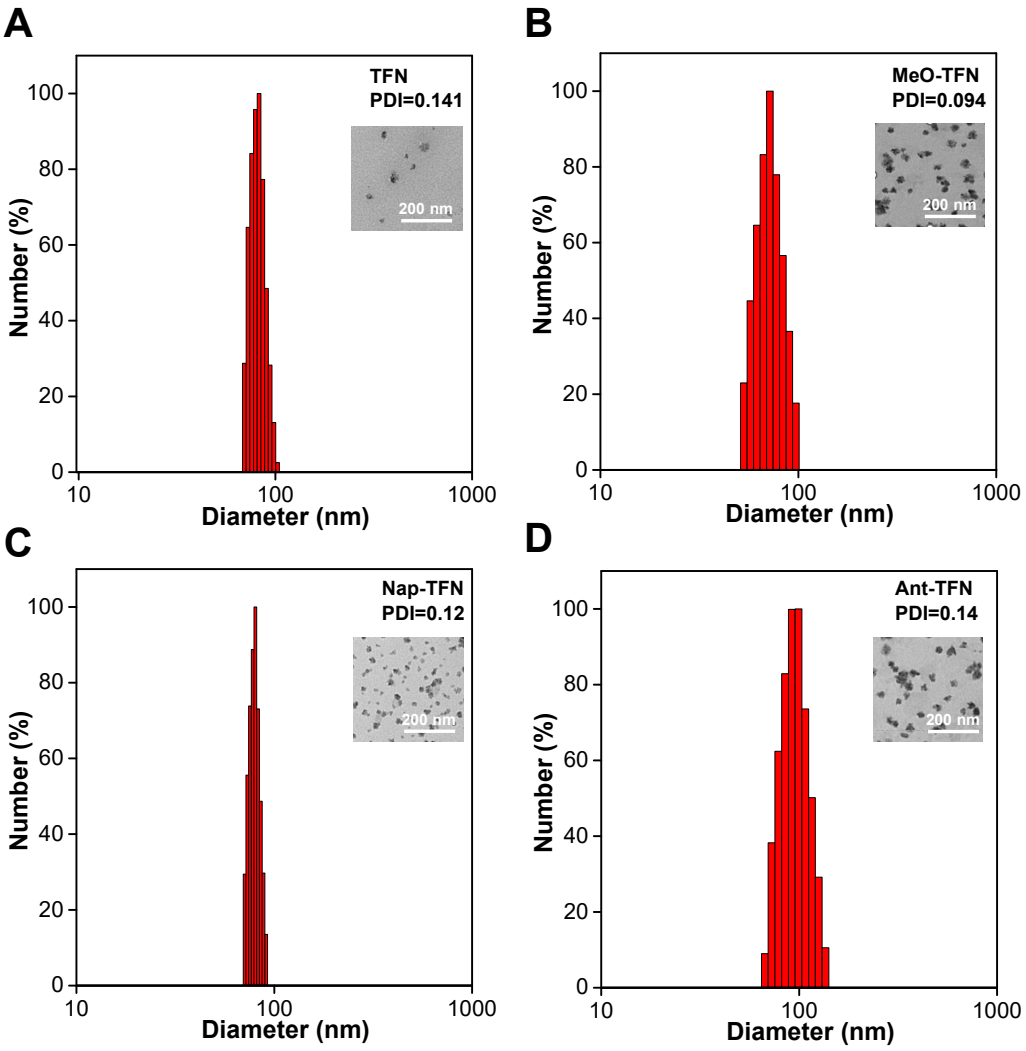

Figure S11. The Dynamic light scattering (DLS) size distribution and transmission electron microscopy (TEM) image (inset photo) of (A) TFN NPs, (B) MeO-TFN NPs, (C) Nap-TFN NPs and (D) Ant-TFN NPs.

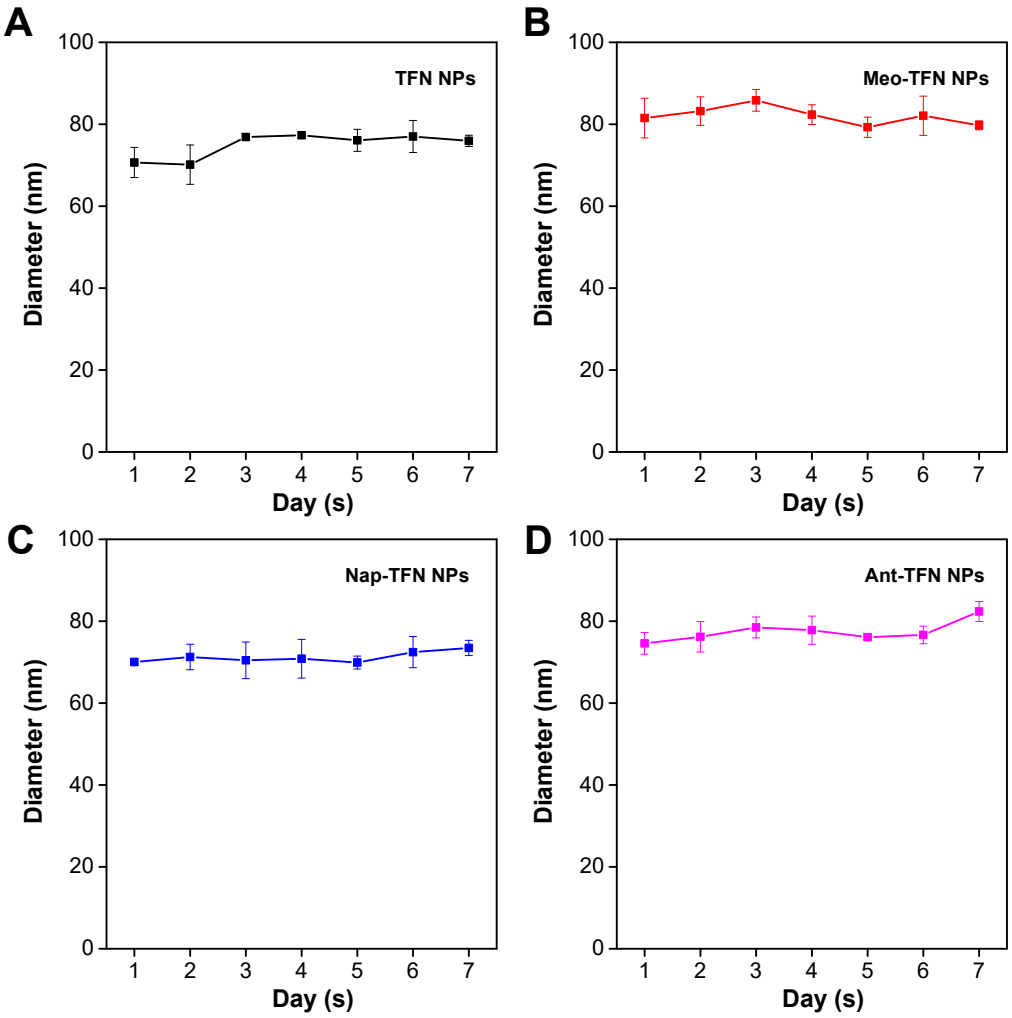

Figure S12. The size changes of (A) TFN NPs, (B)MeO-TFN NPs, (C) Nap-TFN NPs, and (D) Ant-TFN NPs within seven consecutive days, measured by DLS.

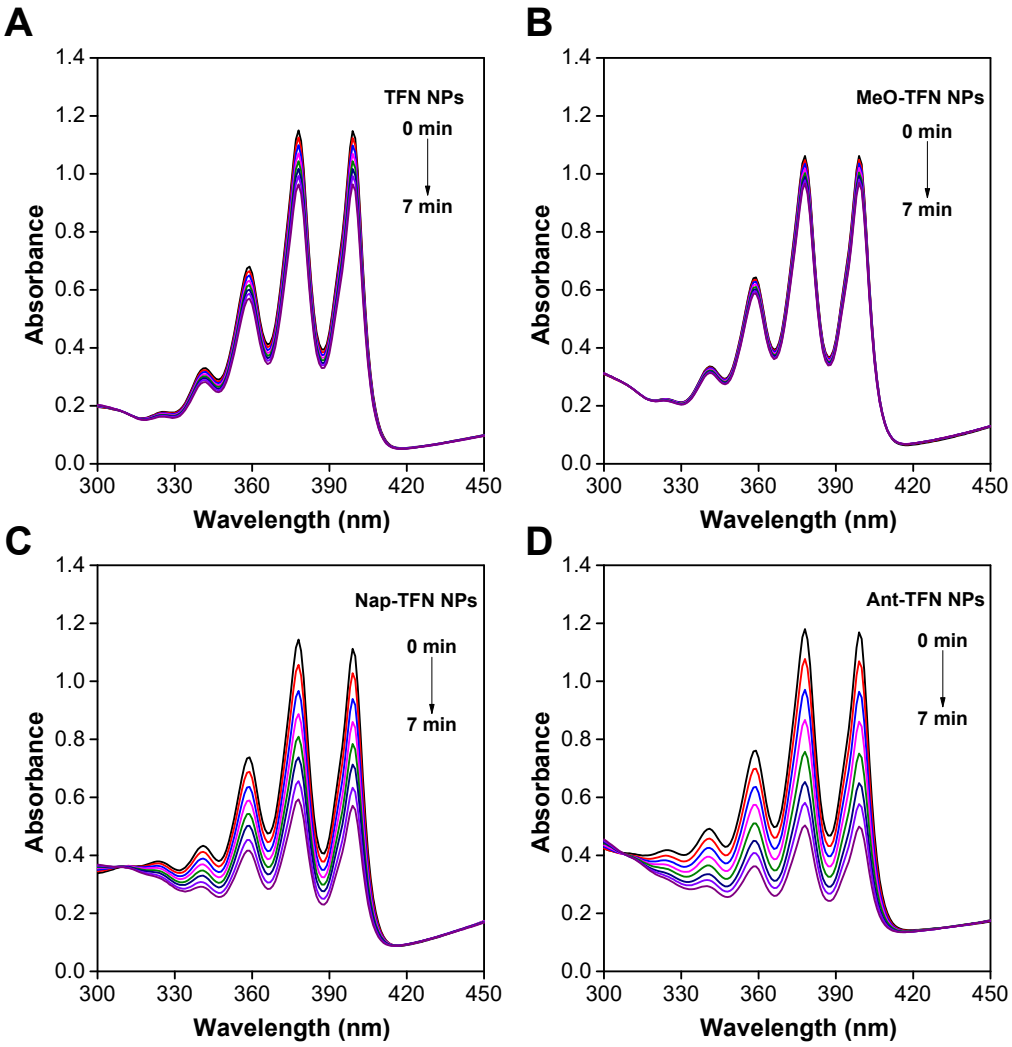

Figure S13. Absorption spectra of the mixed aqueous solution of ABDA (100 μM) with (A) TFN NPs, (B) MeO-TFN NPs, (C) Nap-TFN NPs and (D) Ant-TFN NPs under different time with 60 mW cm^{-2} white light irradiation. (the same concentration of all nanoparticles = 10 μM).

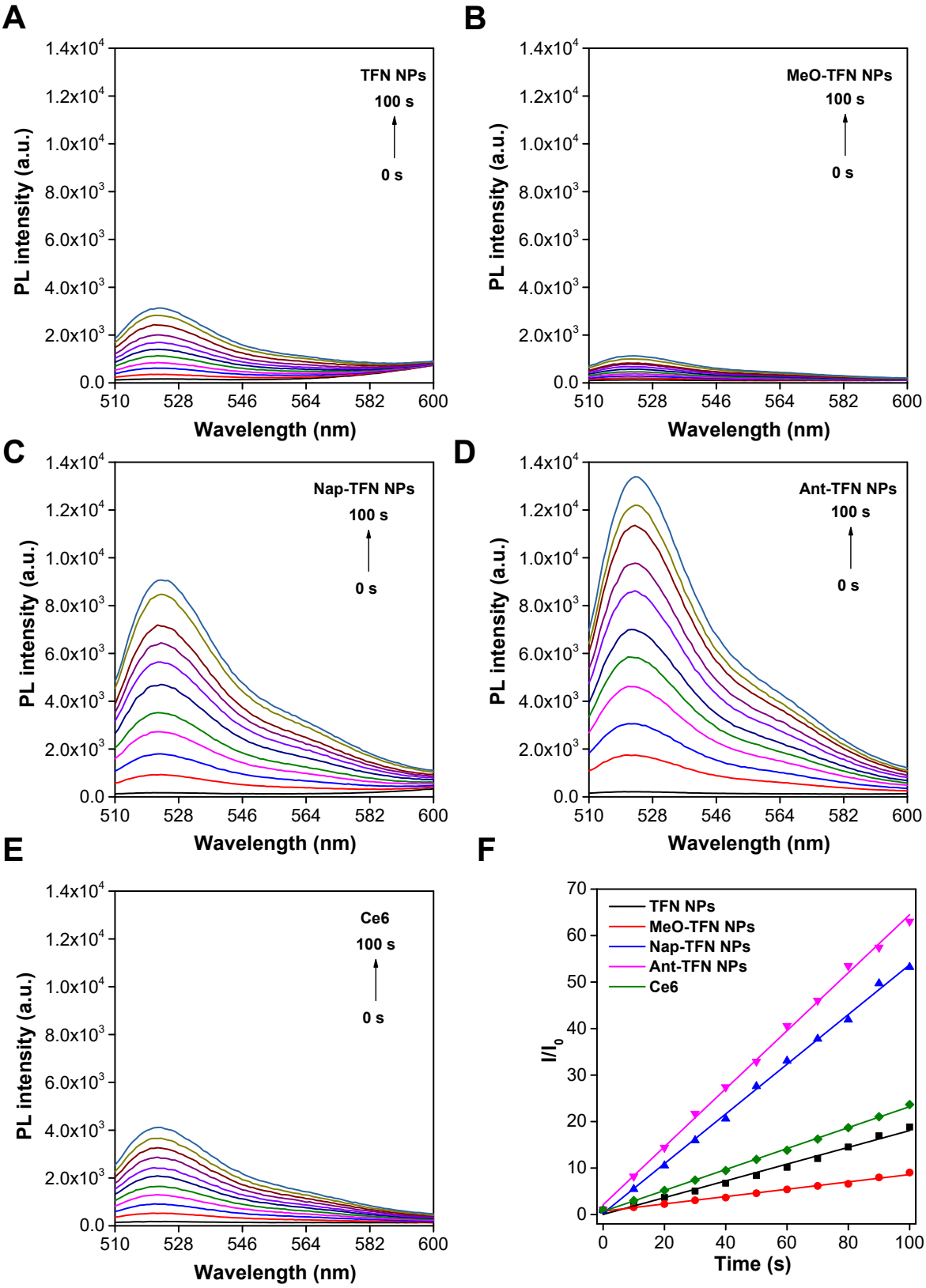

Figure S14. Fluorescence spectra of the mixed aqueous solution of DCFH (5 μM) with (A) TFN NPs, (B) MeO-TFN NPs, (C) Nap-TFN NPs, (D) Ant-TFN NPs, and (E) Ce6 under white light (60 mW cm^{-2}) irradiation. (Concentration of all photosensitizer = 10 μM). (F) Relative fluorescence intensities of TFN NPs, MeO-TFN NPs, Nap-TFN NPs, Ant-TFN NPs, and Ce6 at 523 nm with different irradiation times.

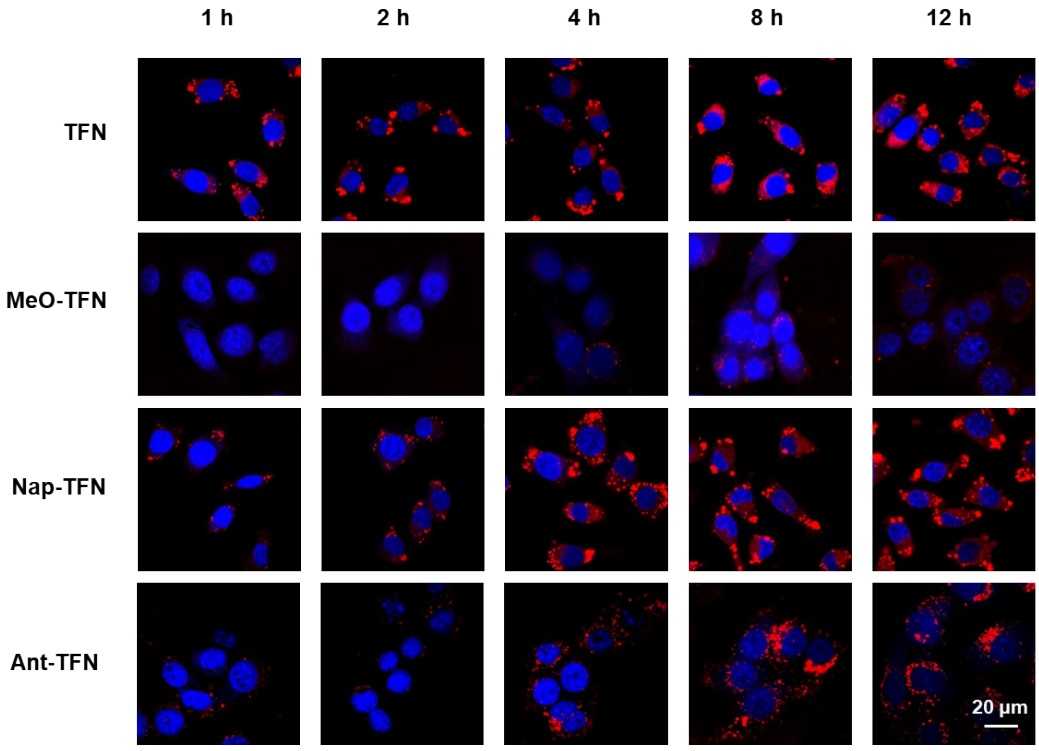

Figure S15. Evaluation of cellular uptake behaviors. CLSM images of 4T1 cells after treatment with TFN NPs, MeO-TFN NPs, Nap-TFN NPs or Ant-TFN NPs (20 μg/mL) for 1, 2, 4, 8 or 12 h.

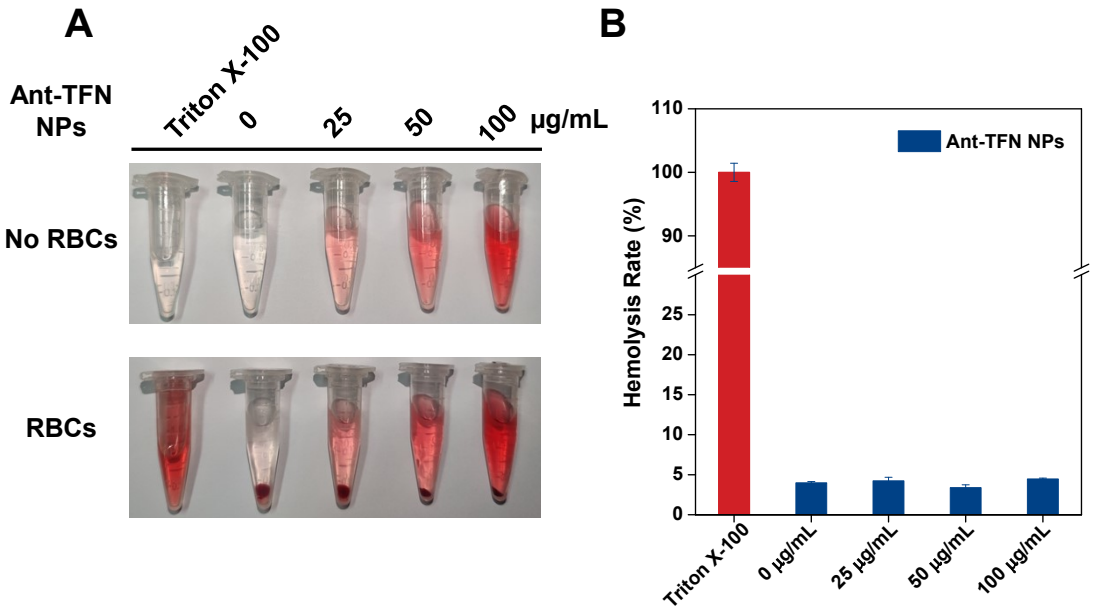

Figure S16. (A) Hemolysis rate of red blood cells after being treated with Ant-TFN NPs at a different concentration from 0 to 100 μg/mL for 3 h at 37 °C, using Triton X-100 as a positive control and nanoparticles in PBS without RBCs as a negative control.

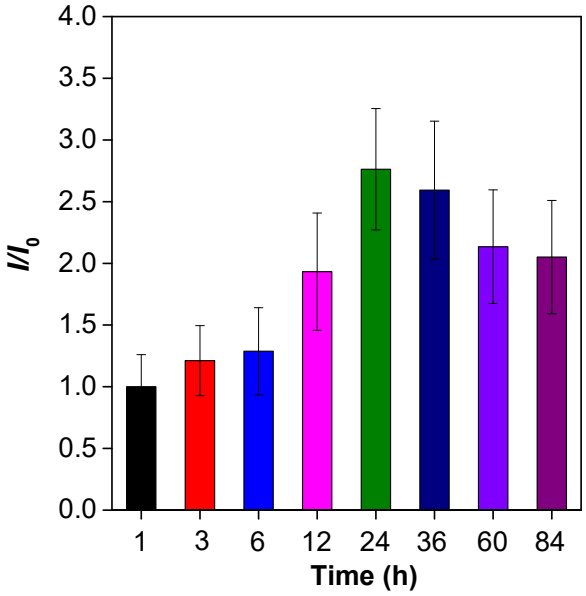

Figure S17. Relative fluorescence intensity of the tumor after intravenously injected with Ant-TFN NPs at different injection time. (I_0 = fluorescence intensity of 1 h post-injection time)

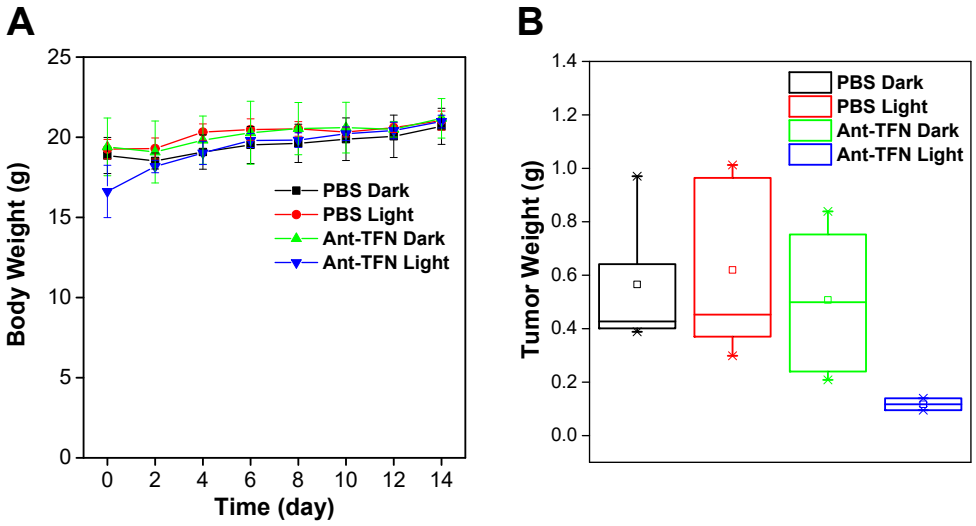

Figure S18. (A) Weight changes of mice in each group. (B) Mean tumor weight of anatomic mice tumor.

Table S2. The results of whole blood test for different groups.[a]

Test	PBS dark	PBS light	Ant-TFN NPs dark	Ant-TFN PSs light	Mice without tumor	Normal Range
WBC(10^9/L)	32.7±6.2	63.9±24.5	41.3±7.2	6.0±3.5	2.9±1.34	0.8-6.8
Lymph#(10^9/L)	28.1±5.2	53.4±18.5	35.8±6.3	5.4±3.46	1.03±0.6	0.7-5.7
Mon#(10^9/L)	1.43±0.3	2.4±0.6	1.5±0.2	0.13±0.06	0.2±0.1	0.0-0.3
Gran#(10^9/L)	3.2±0.8	8.13±5.3	3.9±0.6	0.5±0.1	1.7±1.6	0.1-1.8
Lymph%(%)	85.7±0.9	84.3±2.8	86.6±0.4	87.3±4.7	40.4±26.7	55.8-90.6
Mon%(%)	4..5±0.5	3.7±0.3	3.8±0.05	2.6±1.21	8.6±2.5	1.8-6.0
Gran%(%)	9.8±0.5	11.9±3.1	9.6±0.4	10.1±3.8	50.9±25.8	8.6-38.9
RBC(10^{12}/L)	7.3±0.8	7.1±2.1	6.1±0.5	8.4±1.5	6.73±2.2	6.36-9.42
HGB(g/L)	124.4±14.0	117.7±22.5	106.3±4.1	139.6±17.2	123.3±25.0	110-143
HCT(%)	37.4±6.4	35.9±10.1	30.4±2.5	42.8±2.2	35.5±10.1	34.6-44.6
MCV(fL)	50.8±3.1	51.3±2.2	49.8±0.2	51.8±7.4	53.9±6.6	48.2-58.3
MCH(pg)	16.9±0.6	17.1±2.68	17.4±0.7	16.6±1.2	18.8±2.7	15.8-19
MCHC(g/L)	335.3±26.0	335±41.04	350.6±14.4	325±24.5	352±37	302-353
RDW(%)	17.4±1.5	16.7±2.22	15.2±0.51	18.2±4.7	22.2±1.8	13-17
PLT(10^9/L)	256±64.8	394.7±30.6	224.7±19.3	405±174.7	336.6±210	450-1590
MPV(fL)	6.2±0.3	6.4±0.3	6.4+0.47	6.8±0.2	6.4±0.4	3.8-6.0

[a] White blood cell systems: WBC, Lymph#, Mon#, Gran#, Lymph%, Mon%, Gran%; red blood cell systems: RBC, HGB, HCT, MCV, MCH, MCHC, RDW; blood platelet systems: PLT, MPV.

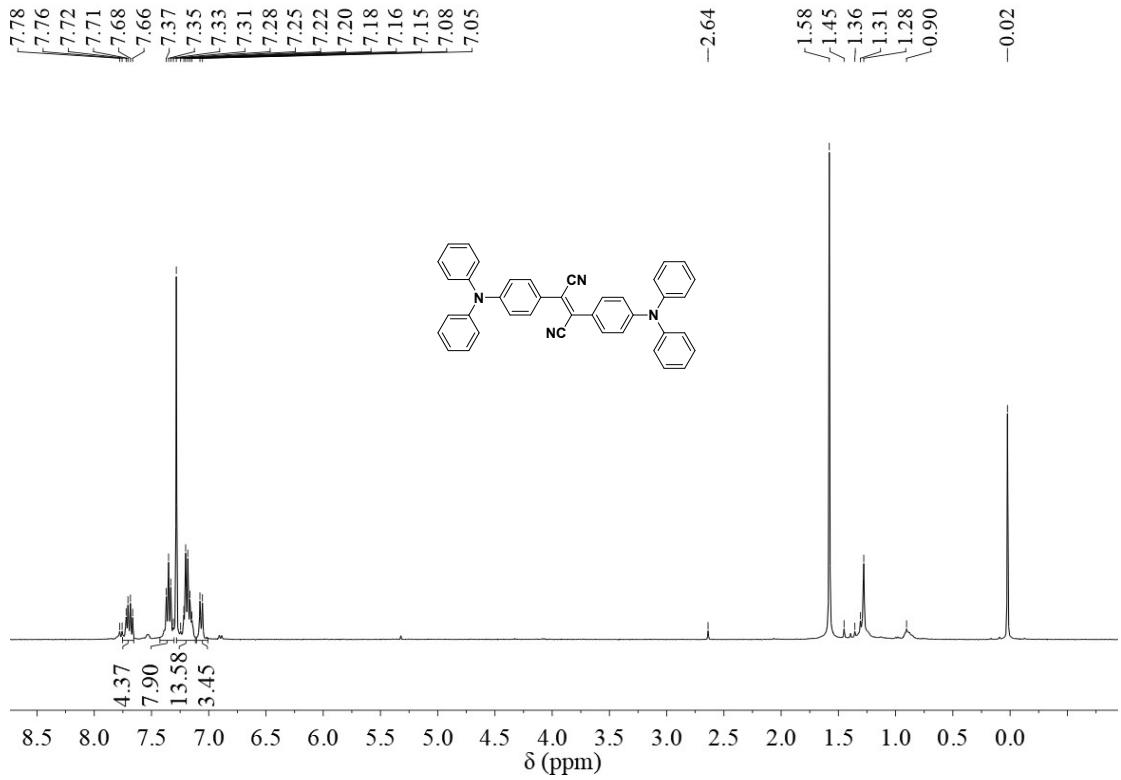

Figure S19. ^{1}H NMR spectrum (400 MHz) of **TFN** in $CDCl_3$.

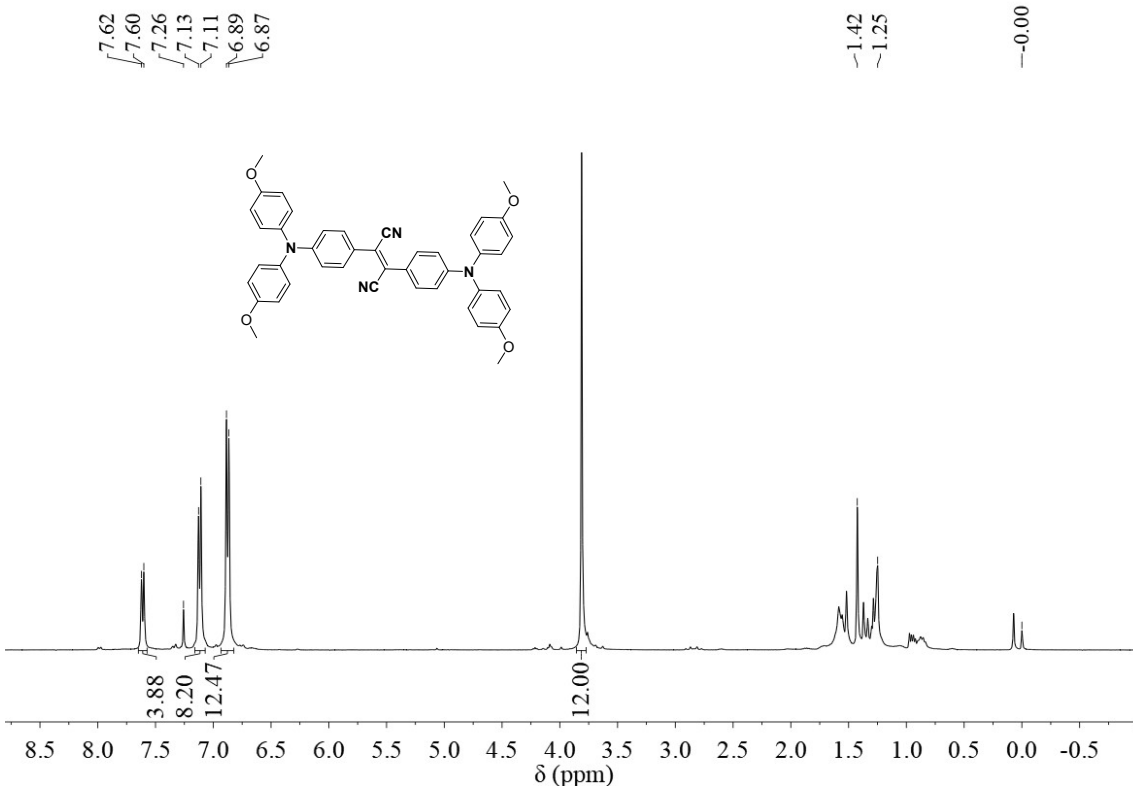

Figure S20. ^{1}H NMR spectrum (400 MHz) of **MeO-TFN** in $CDCl_3$.

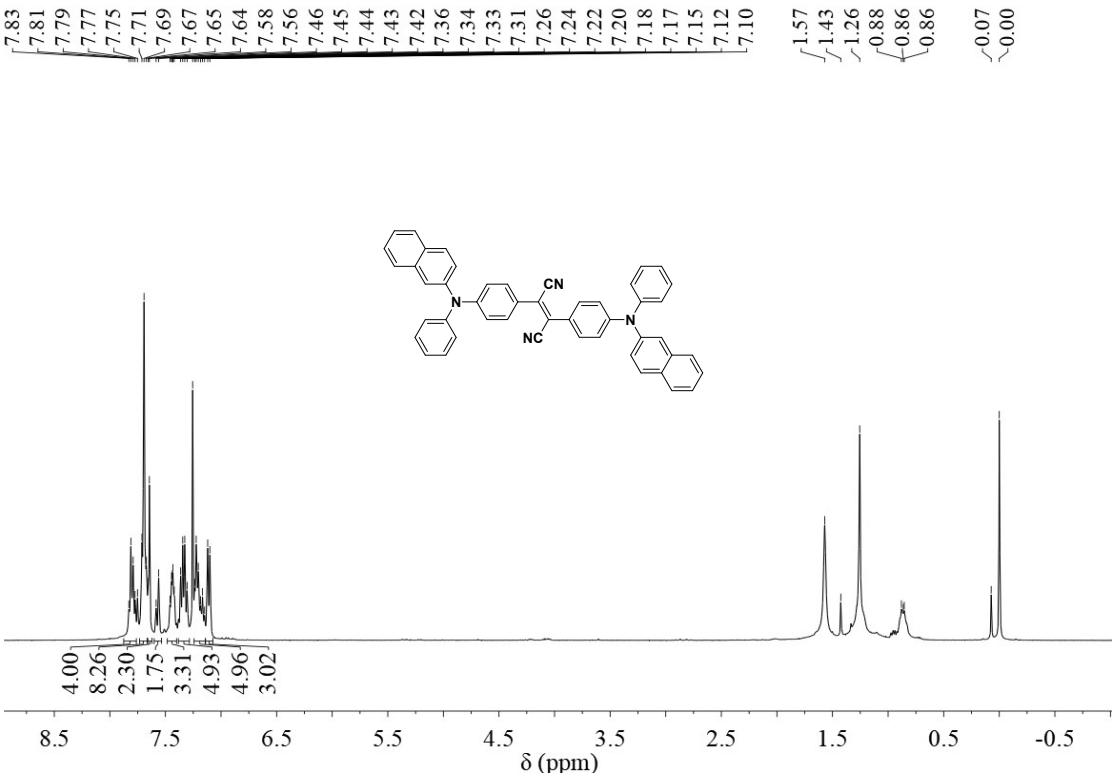

Figure S21. ^{1}H NMR spectrum (400 MHz) of **Nap-TFN** in $CDCl_3$.

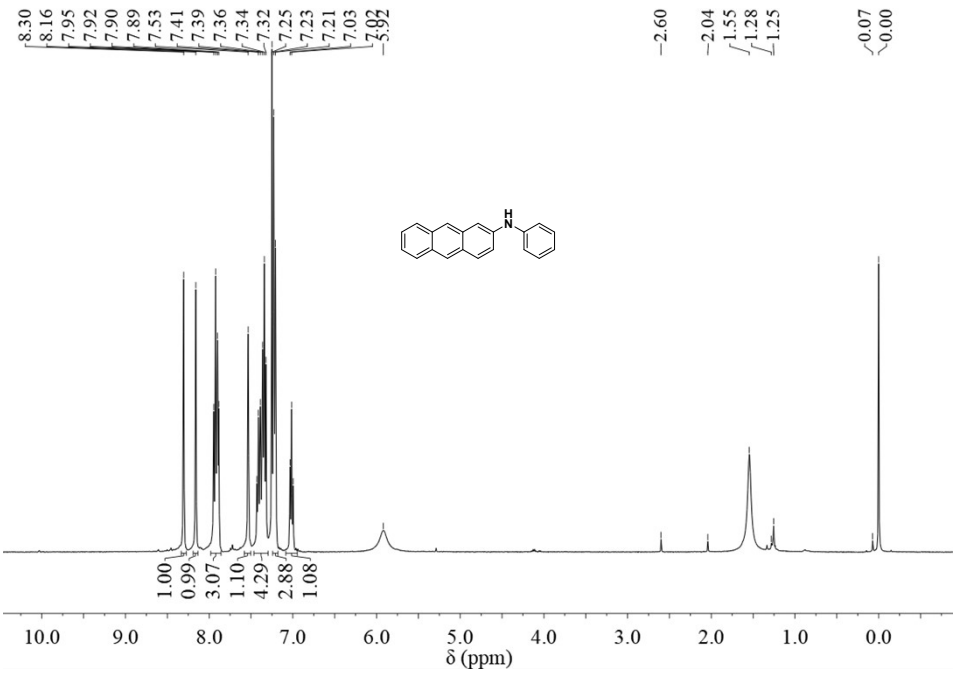

Figure S22. ^{1}H NMR spectrum (400 MHz) of compound ***N*-phenylanthracen-2-amine** in $CDCl_3$.

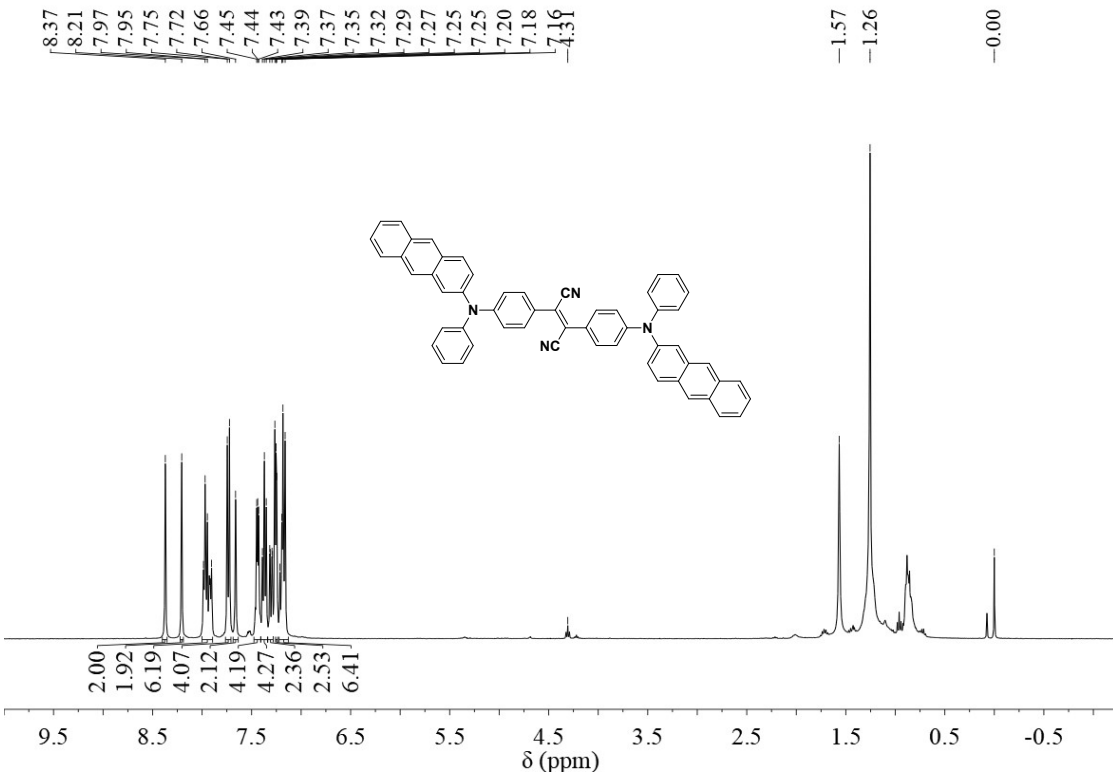

Figure S23. ^{1}H NMR spectrum (400 MHz) of compound **Ant-TFN** in $CDCl_3$.

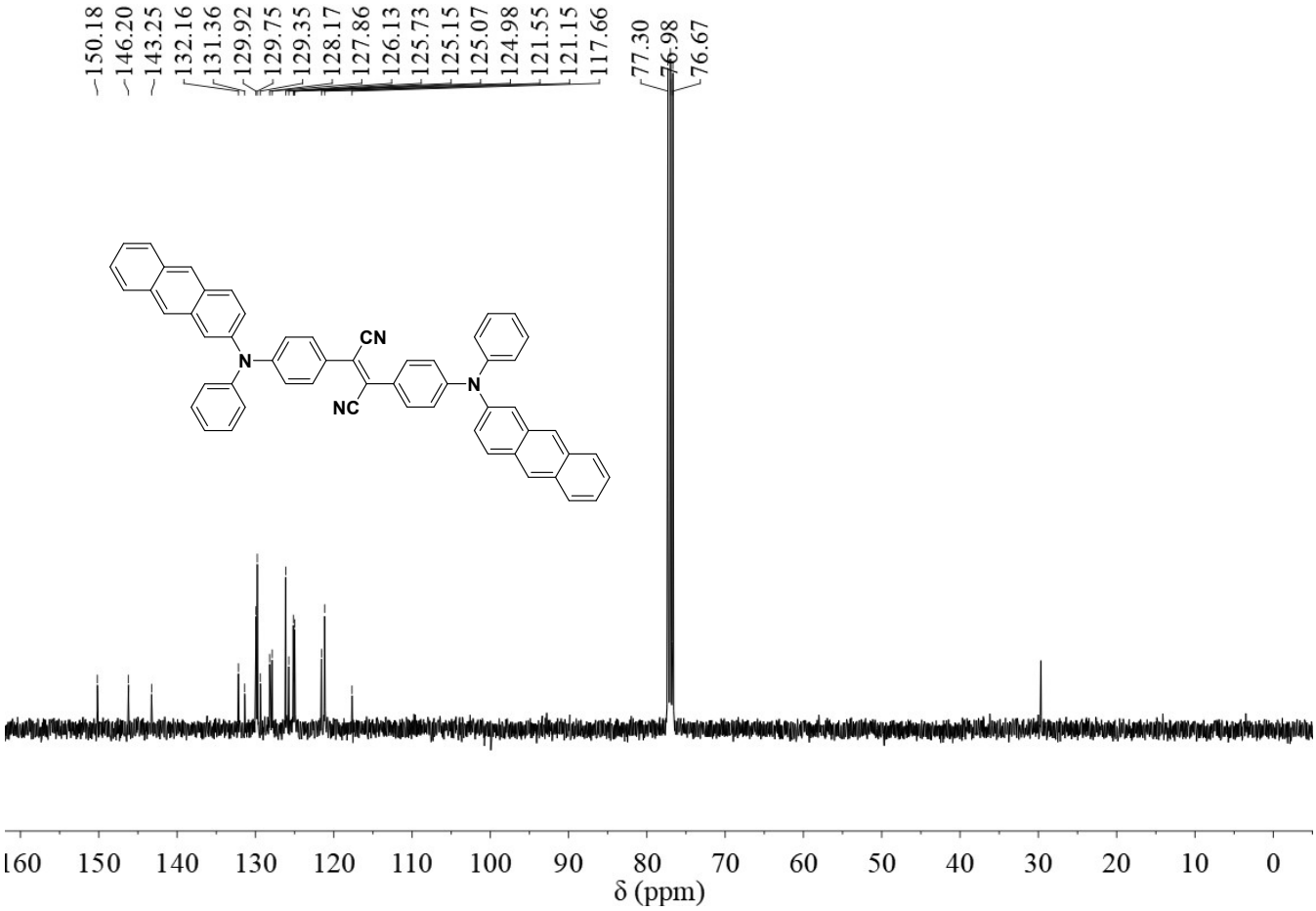

Figure S24. ^{13}C NMR spectrum (400 MHz) of compound **Ant-TFN** in $CDCl_3$.

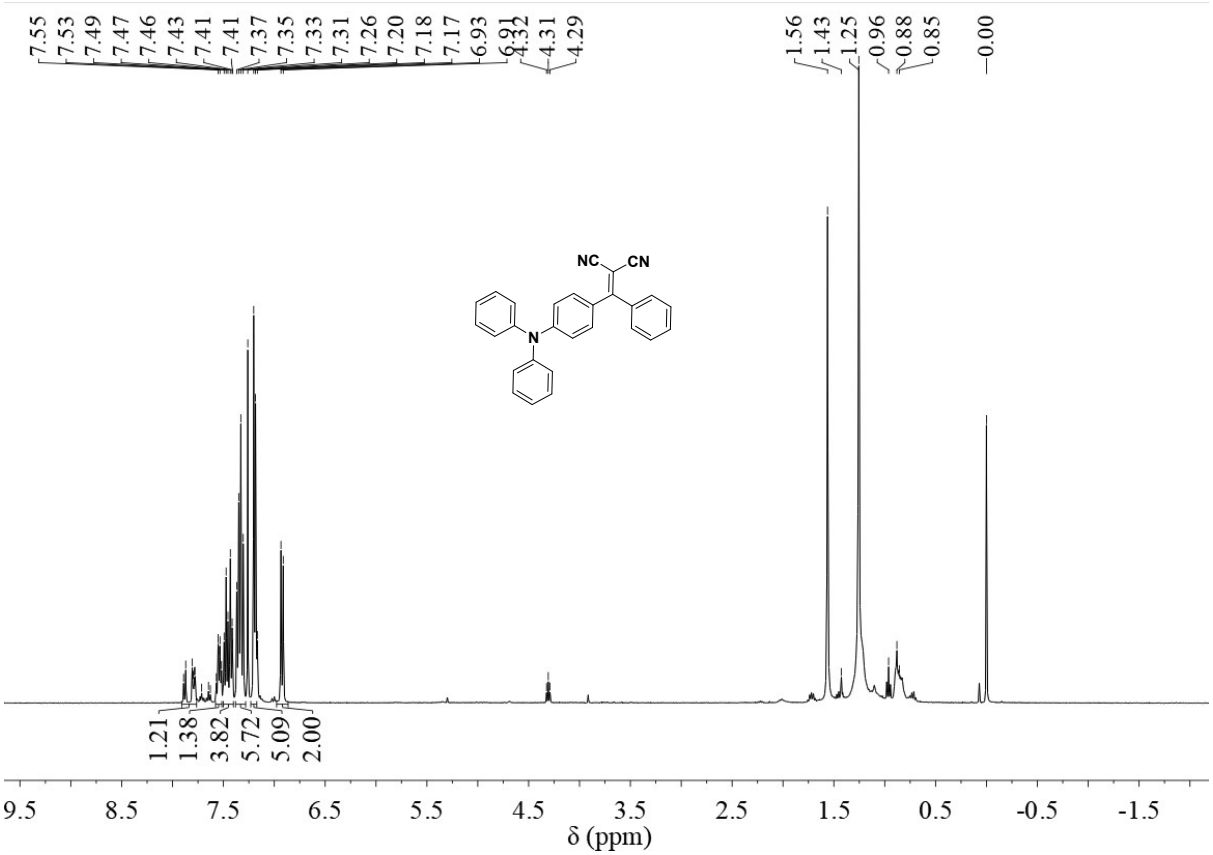

Figure S25. ^{1}H NMR spectrum (400 MHz) of **TMN** in $CDCl_3$.

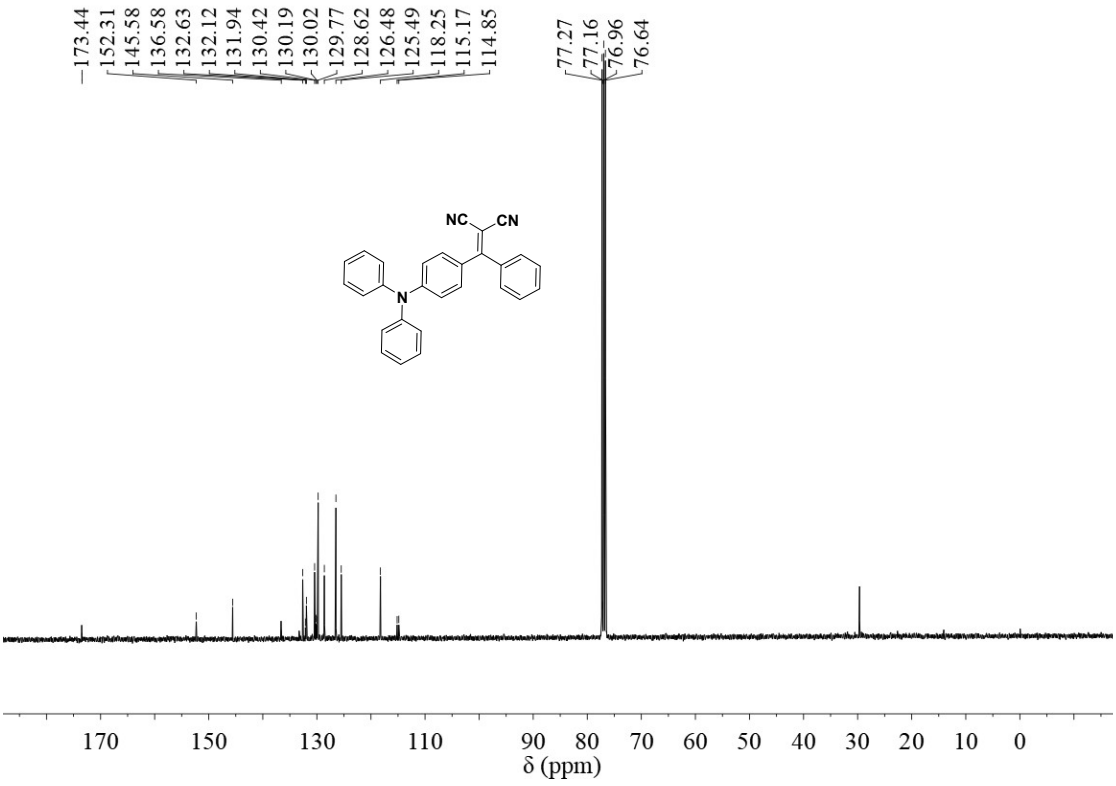

Figure S26. ^{13}C NMR spectrum (400 MHz) of **TMN** in $CDCl_3$.

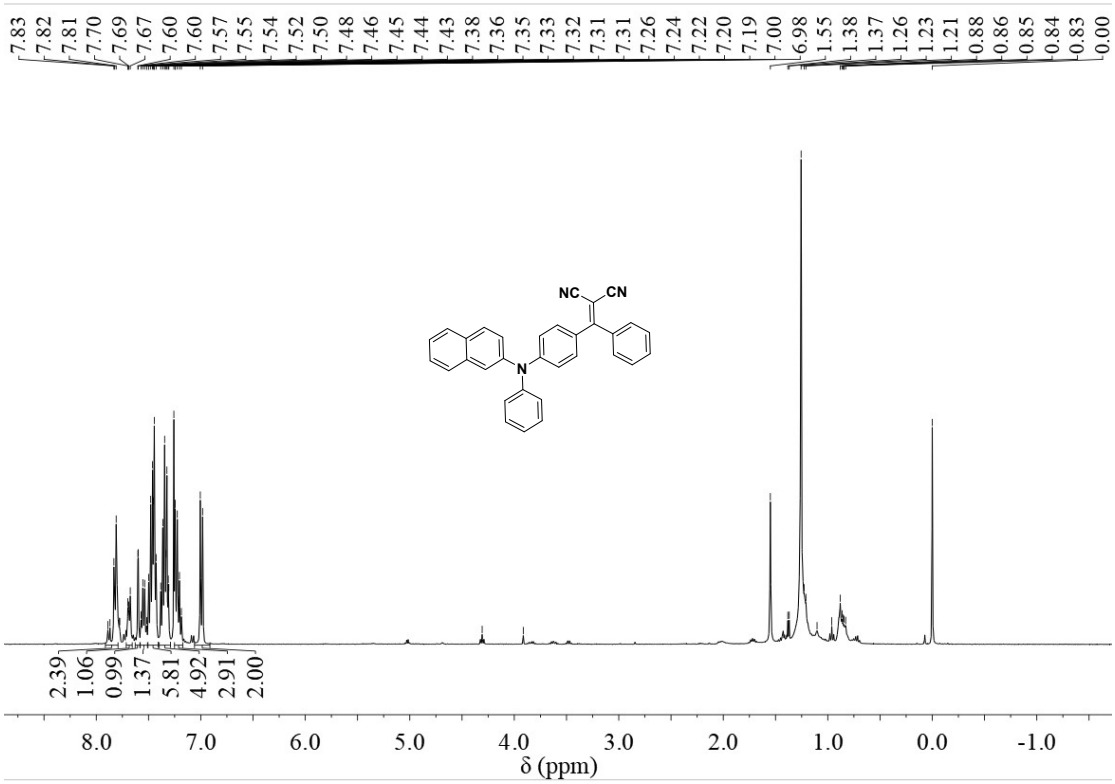

Figure S27. ^{1}H NMR spectrum (400 MHz) of **Nap-TMN** in $CDCl_3$.

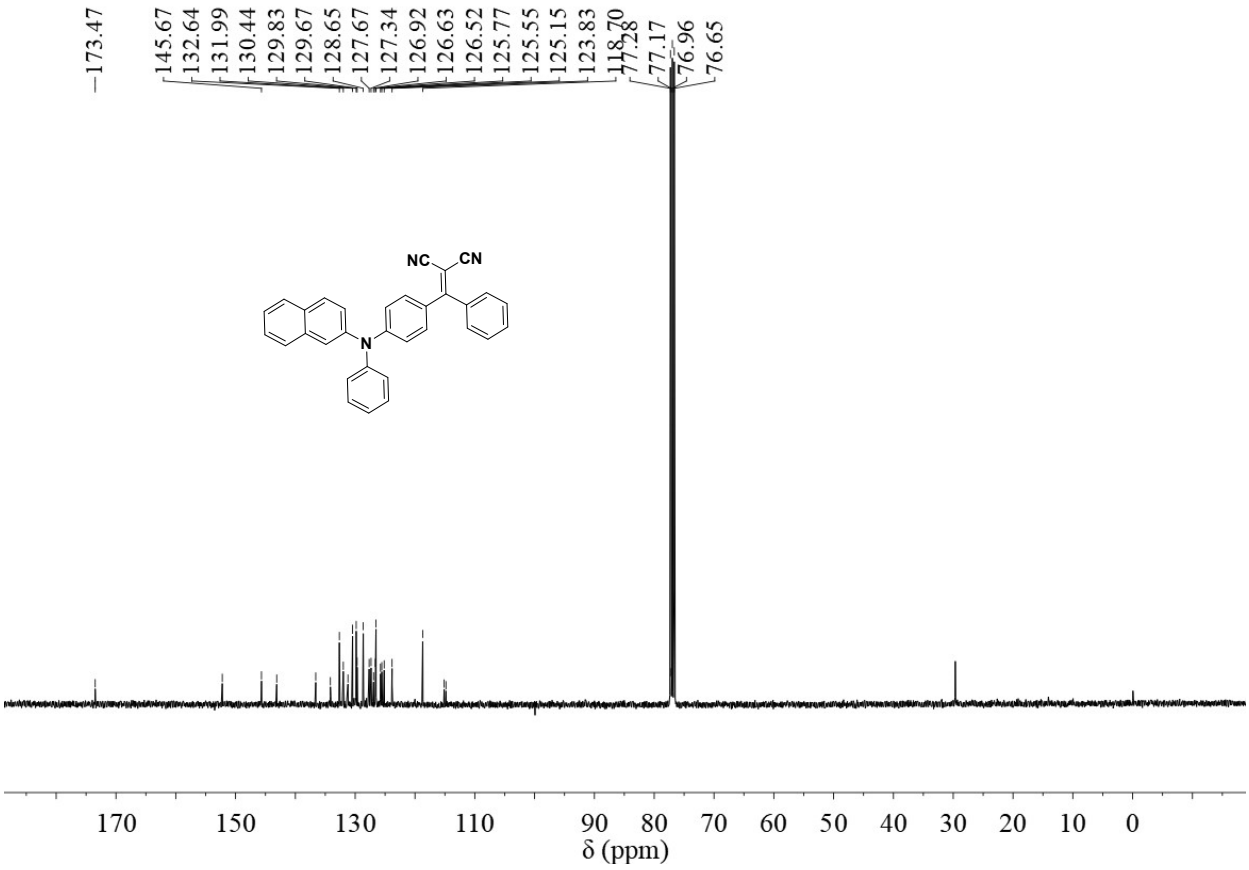

Figure S28. ^{13}C NMR spectrum (400 MHz) of **Nap-TMN** in $CDCl_3$.

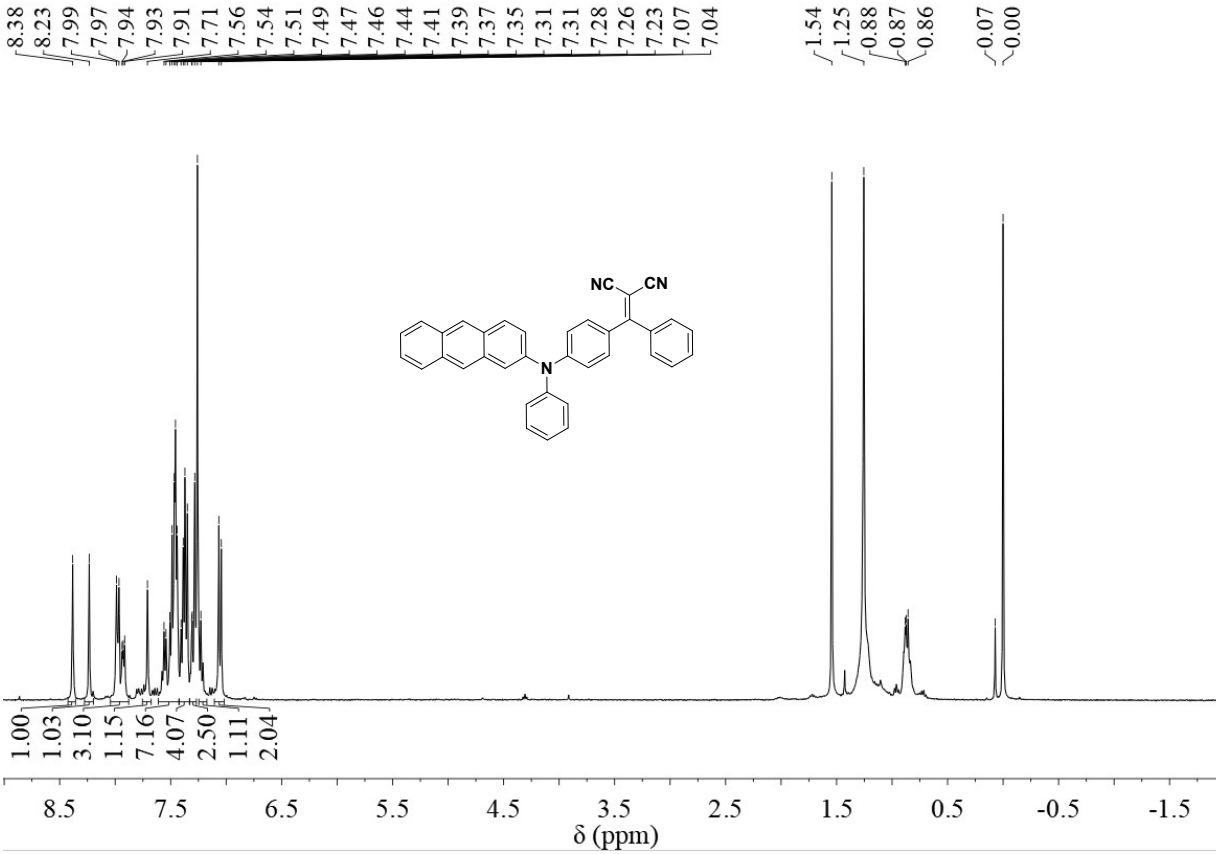

Figure S29. ^{1}H NMR spectrum (400 MHz) of **Ant-TMN** in $CDCl_3$.

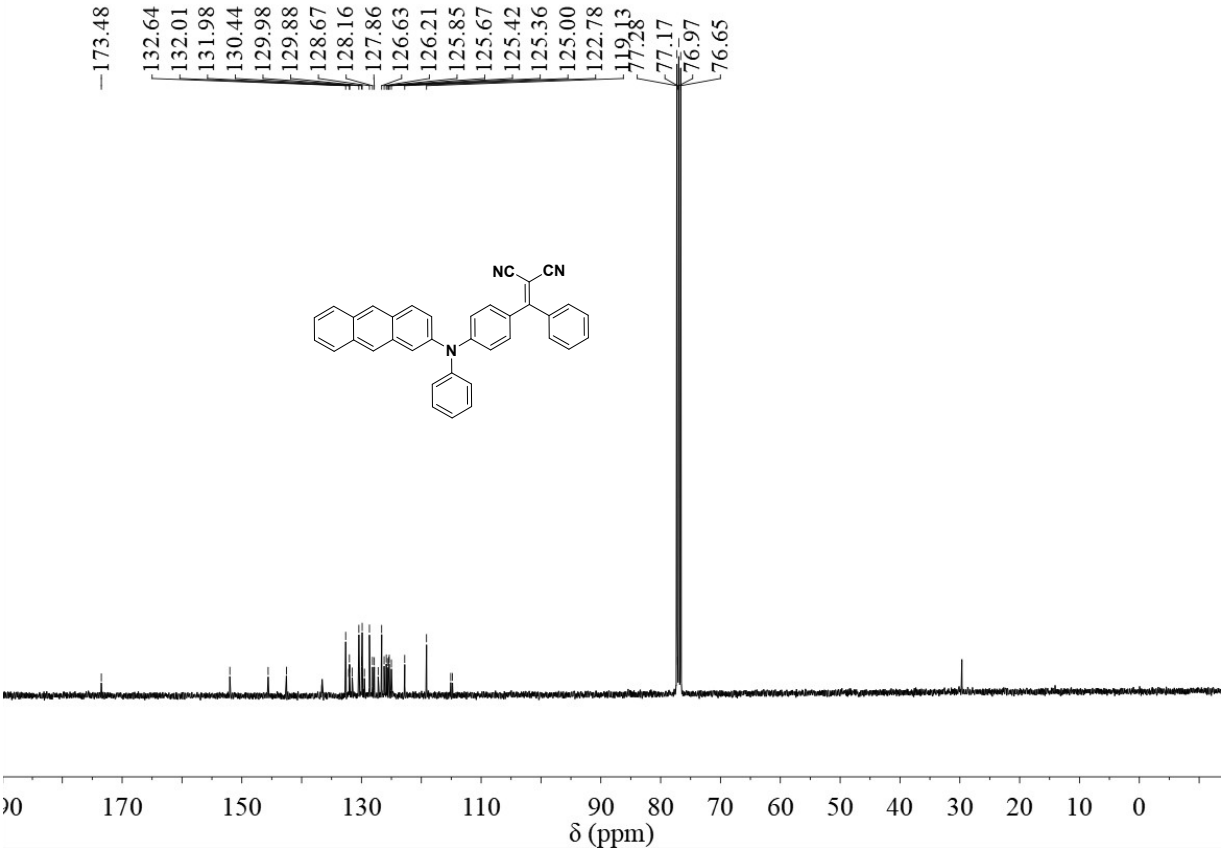

Figure S30. ^{13}C NMR spectrum (400 MHz) of **Ant-TMN** in $CDCl_3$.

References

[1] D. Wu, W. Gong, H. Yao, L. Huang, Z. Lin, Q. Ling, Highly efficient solid-state emission of diphenylfumaronitriles with full-color AIE, and application in explosive sensing, data storage and WLEDs, Dyes Pigm. 172 (2020). https://doi.org/10.1016/j.dyepig.2019.107829.

[2] Z. Liu, F. Liu, Y. Gao, W. Qing, Y. Huang, S. Li, D. Jin, AIEgen Nanoparticles of Arylamino Fumaronitrile Derivative with High Near-Infrared Emission for Two-Photon Imaging and in Vivo Cell Tracking, ACS Appl Bio Mater 2(1) (2019) 430-436. https://doi.org/10.1021/acsabm.8b00643.